The reprogrammed mouse heart phosphoproteome in response to the chronic stress of markedly high cardiac-specific adenylyl cyclase type 8 overexpression

Jia-Hua Qu, Khalid Chakir, Kirill V. Tarasov, Daniel R. Riordon, Maria Grazia Perino, Allwin Jennifa Silvester, and Edward G. Lakatta *

Laboratory of Cardiovascular Science, Intramural Research Program, National Institute on Aging, National Institutes of Health, Baltimore, MD 21224, USA.

Address correspondence to:

Dr. Edward G. Lakatta*

Laboratory of Cardiovascular Science

Intramural Research Program

National Institute on Aging

National Institutes of Health

251 Bayview Boulevard

Suite 100

Baltimore, MD 21224

USA.

Tel: +1 410-558-8202

lakattae@grc.nia.nih.gov

Abstract

An appropriate intensity and duration of increased AC-cAMP-PKA-Ca^{2+} signaling is the quintessential component of acute adaptation to cardiac stress. Our previous work demonstrated the existence of an exquisite heart performance and protection profile in response to chronically increased cardiac AC-cAMP-PKA-Ca^{2+} signaling in young adult mice with cardiac-specific overexpression of adenylyl cyclase type 8 (AC8) (TGAC8). Here, we conducted an unbiased phosphoproteomics analysis in order to determine the role of altered protein phosphorylation in the chronic adaptive heart performance and protection profile of left ventricle (LV) of adult TGAC8 at 3-4 months of age. We identified 12,963 phospho-peptides and 3646 phosphoproteins, including 4990 upregulated phosphopeptides and 781 differentially regulated (741 Up and 40 Down) phosphoproteins in TGAC8 vs. WT. Based on differentially regulated phosphoproteins by genotype, we discovered the enrichment of numerous stress response canonical pathways within reprogrammed TGAC8 LV, including protein kinase A (PKA) signaling, PI3K signaling, and AMPK signaling, predicted upstream regulators, e.g., PDPK1, PAK1 and PTK2B, and downstream functions, e.g., cell viability, protein quality control, and metabolism. In addition to PKA, numerous kinases (83) and phosphatases (30) were hyper-phosphorylated in TGAC8 vs. WT. By combining the phosphoproteome with its proteome and with the previously published TGAC8 transcriptome, we determined which cardiac performance and adaptive protection profiles were coordinately regulated at post-translational modification (PTM) (phosphorylation), translational and transcriptional levels. In order to assess the impact of phosphorylation on mRNA transcription, we determined the phosphorylation states of transcriptional factors (TFs) that differed by genotype. Hyper-phosphorylated TFs in TGAC8 were associated with increased mRNA transcription, and immune responses and metabolism pathways. To determine the coordination of proteome and phosphoproteome in reprogramming the TGAC8 LV, we normalized its phosphoproteome to its proteome (by dividing the protein phosphorylation abundance by protein abundance). In functional enrichment analysis of 229 normalized phosphoproteins that were differentially regulated by genotype, enriched IPA canonical pathways in the phosphoproteome of TGAC8 LV before and after normalization showed high consistency. The combination of aforementioned analyses indicated that many stress response signaling pathways, i.e., PI3K/AKT, ERK/MAPK and ubiquitin labeling, were consistently enriched at transcriptional, translational and PTM levels, and that PI3K/AKT and ERK/MAPK signaling pathways were also activated in the TGAC8 LV. We verified the results via western blot and protein synthesis and degradation detection experiments. Thus, PTM of protein by phosphorylation, per se, contributes immensely to the heart performance and protection profile of TGAC8 LV, and is coordinately regulated with altered transcription and translation in the TGAC8 to activate critical stress response pathways.

Keywords

left ventricle, adenylyl cyclase 8, AC-cAMP-PKA-Ca^{2+} signaling, phosphoproteome, proteome, transcriptome, PI3K/AKT signaling pathway.

Introduction

Cyclic AMP (cAMP) is a pivotal second messenger, which exerts multifaceted effects on most significant physiological processes, such as cardiac contractility, glycogenolysis and lipolysis, hormone release, etc[1]. In mammalians, there are nine transmembrane adenylyl cyclase (AC) (mAC) isoforms (AC1-9) and one soluble AC (sAC, also called AC10) catalyzing the conversion of ATP into cAMP[2], which usually activates the phosphorylation cascade, serving as the central motif of cellular signaling[1,3]. Increased AC-cAMP-PKA-Ca^{2+} signaling is the quintessential component of both acute and chronic cardiac responses.

AC8, the isoform, is highly expressed in brain regions[2,4]. Unlike two dominant cardiac AC isoforms, AC5 and AC6, which are inhibited by intracellular Ca^{2+} and inhibited in heart failure (HF), AC8 is stimulated by Ca^{2+}-calmodulin (CM)[5,6] and involved in nervous system functions, like learning and memory[2,4]. Our lab and others have demonstrated that cardiac-specific overexpression of AC8 (TGAC8) markedly increases the heart rate and ejection fraction, similar to acute exercise but chronic and in the absence of corporal exertion, and persists on a 24 hours per day and 7 days per week basis[5,7-9]. Despite this persistent high-level of heart performance driven by markedly elevated level of AC8-cAMP -PKA-Ca^{2+} signaling, which usually proceeds to near-term cardiac dysfunction, the TGAC8 survives for an extended period of time, up to about a year of age without excessive mortality.

It is of utmost importance to unravel how the TGAC8 adapts the heart to this chronic stress, as this knowledge can be applied to the study of cardiac physiology and pathology and even to develop treatments for cardiovascular diseases (CVDs). In this regard, as a first “port-of-call”, we had recently compared the LV transcriptome and proteome in TGAC8 and WT littermates[10]. Because PKA signaling pathway was highly enriched in TGAC8 vs. WT, we reasoned that protein phosphorylation will differ between TGAC8 and WT, and the phosphorylation modification will play a crucial role in the remarkable adaptation capacity of the TGAC8 heart in response to markedly increased AC8-cAMP-PKA-Ca^{2+} signaling. We have assessed the concordance of the genotypic differences at the phosphorylation level to some degree in western blot (WB) experiments[10].

As the body is a quite complex system, regulation at a single level cannot reveal the whole picture in an organism, and multiple levels of regulatory mechanisms are coordinated to defend against stimuli and maintain health[11]. Phosphorylation is one of the most important and most extensively studied post-translational modifications (PTMs) on proteins. Various kinases and phosphatases within cells phosphorylate and dephosphorylate a myriad of proteins respectively to regulate their activities and affect multiple signaling pathways. In the present research, we conducted Tandem Mass Tag (TMT)-labeling MS of left ventricular samples of the three-month old male TGAC8 and WT mice, to unravel the reprogrammed phosphoproteome and proteome of the TGAC8 left ventricle (LV). In addition, by comparing genotypic differences in the proteome and phosphoproteome of the present study with genotypic differences in transcriptome published

previously[10], we sought to determine whether some adaptive mechanisms that emerge in the TGAC8 LV are regulated at transcriptional, translational and PTM (phosphorylation) levels.

Materials and Methods

1. Animals.

The cardiac-specific overexpression of AC8 (TGAC8) mouse, generated by inserting a cDNA coding for human AC8 after the murine α-myosin heavy chain promoter, was a gift from Nicole Defer/Jacques Hanoune, Unite de Recherches, INSERM U-99, Hôpital Henri Mondor, F-94010 Créteil, France. The 12-week old male TGAC mice were used as study cases, and age matched WT littermates, in the C57/BL6 background, were used as controls. All studies were performed in accordance with the Guide for the Care and Use of Laboratory Animals published by the National Institutes of Health (NIH Publication no. 85-23, revised 1996). The experimental protocols were approved by the Animal Care and Use Committee of the National Institutes of Health (protocol #441-LCS-2016).

2. Isolate and store mouse heart.

Three-month old male C57 mice (TGAC8 and WT) were euthanized and the heart was isolated. The left ventricle (LV) tissues were extracted and stored in tubes at -80°C.

3. Mass spectrometry for phosphoproteome and data process.

Four TGAC8 LVs and five WT LVs were sent to National Heart, Lung, and Blood Institute, National Institutes of Health, Bethesda to conduct mass spectrometry using the standard tandem mass tag (TMT) labeling method to obtain the phosphoproteome and total proteome concurrently in the same platform. The raw data were processed in Proteome Discover (ThermoFisher Scientific, software version 2.2). After filtering low quality signal, we remained the medium and high confidence peptides. For total proteins and phosphoproteins, we combined peptides to computed the normalized/standardized expressions with the default parameters. Then we divided the expressions of phosphoproteins to those of total proteins to obtain the normalized phosphoproteome. As the expressions appeared to be near normal distribution, we calculated the fold change by dividing the average value of TGAC8 samples by the average value of WT samples, and calculated p-value using two-sided unpaired Student's t-test.

4. Analyses of the TGAC8 LV transcriptome.

The processed transcriptomic data were obtained from our recently published work (ref). The significantly changed mRNAs (TGAC8 vs. WT, q-value < 0.05) were uploaded into DAVID[2] (version: 6.8; https://david.ncifcrf.gov/home.jsp) for Gene Ontology (GO) term enrichments, and were also imported into Ingenuity Pathway Analysis[3] (IPA (QIAGEN, March 2020)) for upstream kinases and phosphatases prediction. Kinases and phosphatases were selected from the transcriptome and their changes at mRNA level were displayed to observe their regulation by the overexpression of AC8.

5. Analyses of phosphoproteome.

Both unnormalized and normalized phosphoproteome were analyzed and visualized in PCA, heatmap, and volcano plots. With the cutoff -log(p-value) > 1.3 and absolute(log2(fold change)) ≥ 0.4, we obtained the significantly changed unnormalized and normalized phosphoproteins (TGAC8 vs. WT) and imported them into IPA for functional analyses respectively, and compared the canonical pathway enrichments from these two datasets. In IPA, the upstream kinases were predicted based upon the unnormalized phosphoproteom, and the regulatory pathways from the predicted upstream kinases to downstream effective signaling pathways were generated. Molecular and cellular functions were also enriched in IPA. The similar analyses to those conducted in the TGAC8 LV transcriptome were also done in the TGAC8 LV total proteome to observe the GO term enrichment, predicted activities of upstream kinases and phosphatases, and expression of kinases and phosphatases at protein level.

6. Analyses of phosphopeptides.

The upregulated phosphopeptides (TGAC8 vs. WT, p-value < 0.05 and log2(fold change) > 0) were processed in R. After split of peptides with multiple phosphosites into individual peptides and filtration of ambiguously identified sites, 2264 phosphopeptides were selected. Protein peptide sequences of full length were downloaded from Uniprot database[12] and matched to the protein accessions corresponding to processed and selected phosphopeptides. Peptides centered on the phosphosites and flanked by 6 amino acids on the N and C termini respectively were extracted from the matched protein peptide sequences, and uploaded into WebLogo[13] (http://weblogo.threeplusone.com/) and iceLogo[14] (https://iomics.ugent.be/icelogoserver/) for sequence motif analysis. In WebLogo online analysis, different amino acids were labeled in different colors representing different chemical properties (refer to figure legend). In iceLogo online analysis, a public amphiphilicity index of polar amino acids reported by Mitaku and colleagues[15] was used as an aid to characterize the amino acid preference at membrane-water interfaces. In addition, the phosphopeptides of PI3K/Akt substates were summarized and displayed in stacked bar plots.

7. Integrative analyses of transcriptome, proteome and phosphoproteome.

The changes of significantly regulated molecules (TGAC8 vs. WT, q-value or p-value < 0.05) in transcriptome, total proteome, and unnormalized phosphoproteome were displayed in circos plot. In addition, the changes at different level were compared and visualized in correlation scatter plots. The discordant proteins whose changes directions in total proteome and phosphoproteome were opposite were used to analyze the specific regulation at the phosphorylation level by the use of Reactome and GO (Cellular component and biological process) databases.

As to the coordinated regulation, the above mentioned significantly regulated molecules (TGAC8 vs. WT) in each dataset were imported into IPA for canonical pathway enrichment. PI3K/AKT signaling and protein ubiquitination were two coordinated pathways across all omics. The phosphopeptides of protein substrates of PI3K were extracted from the phosphopeptide dataset and the numbers of changed phosphopeptides (TGAC8 vs. WT) were summarized and visualized in stacked bar plot. The PI3K/AKT signaling pathway were visualized in IPA, and nodes in the pathways were marked in different colors in terms of their changes at different levels.

As kinases and phosphatases are pivotal in phosphorylation, and transcription factors (TFs) are important in transcription regulation, they were extracted from transcriptome, proteome, and phosphoproteome to observe their changes (TGAC8 vs. WT) and deduce their role in the reprogram of phosphoproteome. The upstream transcription regulators including but not only TFs were predicted on the basis of transcriptome and proteome by the utilization of knowledge base in IPA, and their expressions were searched in multiple datasets. Furtherly, TFs that were significantly regulated at phosphorylation level (TGAC8 vs. WT, p-value < 0.05) were defined as significantly changed phosphorylated TFs in this research, and they were uploaded into STRING database[4] (version: 11.0; http://string-db.org/) to generate protein-protein interaction network and enrich KEGG pathways. They were also imported into IPA for canonical pathway, molecular and cellular functions enrichments.

8. Data process and graphics production.

Most raw data were precleared and processed using RStudio (version: 1.1.463) in R language (version: 3.5.3), in which the tidyr package and dplyr package were applied. In addition, GraphPad Prism (version: 7), Microsoft Excel (version: 2019) and Adobe Illustrator (version: CC 2019) were also used for statistics and graphics. Venn diagrams were generated in Venny[5] (version: 2.1.0; http://bioinfogp.cnb.csic.es/tools/venny/index.html). Circos plot was generated using Circos software[6] in Perl language.

Results

1. The TGAC8 reprograms the LV phosphoproteome.

The TMT-labeling quantitative MS identified **12,963 phospho-peptides** (File 1: Sheet 1) and **3646 phosphoproteins** (File 1: Sheet 2). The principal component analysis (PCA) (Figure 1A) of the 3646 phosphoproteins in each mouse showed that the TG and WT samples were distinguished into two groups completely. The heatmap (Figure 1B) showed the intra-group consistency of upregulated phosphoproteins in TGAC8 compared to WT. Within the cutoff at -log10(p-value) > 1.3 and absolute value of log2(fold-change(TG/WT)) ≥ 0.04, 781 phosphoproteins were differentially regulated by genotype. Of the 781 phosphoproteins, the phosphorylation levels of 741 proteins were increased and only 40 were decreased in the TGAC8 vs. WT LV (Figure 1C).

2. Functional analyses of the phosphoproteome.

We performed the canonical pathway, upstream regulation, and downstream function analyses of the remodeled LV phosphoproteome of TGAC8 using the Ingenuity Pathway Analysis (IPA) software.

2.1. Canonical pathway analysis of the remodeled LV phosphoproteome of TGAC8.

To study the mechanism at phosphorylation level, we first performed canonical pathway analysis using IPA. Top canonical pathways within the phosphoproteome that were statistically differentially enriched in TGAC8 vs. WT were displayed in the bar plot (Figure 1D and File 2: Sheet 1). Of these pathways, cardiac hypertrophy signaling (enhanced) is most highly activated (z-score as high as 4.867) (Figure 1D). The combination of Supplementary Figure 1 and File 2: Sheet 2 and our recently published work[10] showed that the phosphorylation status of numerous molecules, e.g., Ca^{2+} ATPase, RyR2, Ncx, involved in excitation, calcium cycling, contraction, relaxation and protein synthesis, was elevated in the TGAC8 vs. WT LV. However, we have demonstrated that at three-month of age, the mouse age in the present study, the LV mass is not elevated in TGAC8 vs. WT[10]. Of note, transcriptomic, proteomic and WB analyses indicated that pathologic hypertrophic markers were not increased in TGAC8 vs. WT[10]. In this regard, the activation of key stress response signaling pathways, e.g., protein kinase A (PKA) signaling, PI3K signaling, and AMPK signaling, may protect against pathological changes, that result in an increase in cardiac mass in TGAC8 despite its chronic increase in performance. For example, activated PKA signaling can restrict the activity of AC8, acting as a feedback to fine-tune the downstream signaling networks inside the body[3]. Additionally, nitric oxide (NO) signaling may coordinate cardiac protection in the increase in cardiac mass (Figure 1D). Increased phosphorylation status of HSP90 and Akt in TGAC8 synergistically increase eNOS activity[16], and increased NO produced by eNOS may modulate the function of the ryanodine receptor Ca^{2+} release channel (RyR2), which was increased on the PKA dependent phosphopeptides in TGAC8,

on the cardiac sarcoplasmic reticulum[17]. The TMT-labeling MS identified significant upregulated phosphorylation in the peptides of RyR2 (RISQTSQVSIDAAHGYSPR, E9Q401 [2805-2823]) (File 1: Sheet 1) , consistent with the PKA induced phosphorylation of RyR2-S2809 mediating the increase in Ca^{2+} spark amplitude[18].

2.2. Upstream regulators of the remodeled LV phosphoproteome of TGAC8.

As known, the overexpression of AC8 activates the AC8-cAMP-PKA phosphorylation axis[9]. There were 2264 phosphosites whose names and locations are unambiguous within the 4990 upregulated phosphopeptides (p-value ≤ 0.05 and log2(fold-change(TG/WT)) ≥ 0) in TGAC8 vs. WT. The majority of these phosphosites were serines (S) and threonines (T), and a few were tyrosines (Y) (Figure 2A). By using WebLogo, we profiled the phosphorylation motif sequences (Figure 2B). A typical AKT substate motif, R-X-X-pS/T, was the most abundant substrate motif, consistent with increased PKA dependent phosphorylation[19,20]. In addition to S and T, the center phosphosites also included phosphotyrosine (Y). The center phosphosites were mainly flanked by the P-E-E sequence on the C terminus, endowing a strong hydrophobic and acidic property to the C terminus of the substrate sequences (Figure 2B), supported by the amphiphilicity index analysis in iceLogo (Figure 2C). Because phosphorylation substrate motifs were not restricted to PKA's substrate motif, additional kinases must be also involved in reprogramming the TGAC8 phosphoproteome. Therefore, we were inspired to explore additional kinase-substrate pathways mediating the effect of the cardiac-overexpression of AC8 here.

IPA predicted that 26 kinases were responsible for the above-mentioned phosphorylation motifs (File 2: Sheet 3), among which, three had previously been identified to differ by genotype in the LV transcriptome, 18 were previously shown to differ by genotype in the LV proteome, and 18 were identified in the present phosphoproteome. Of note, most of the identified kinases were upregulated in TGAC8 vs. WT at transcription, translation and PTM (phosphorylation) levels. Within the phosphoproteome, eight kinases were predicted to be differentially activated by genotype, and the phosphorylation level of four of these (PDPK1, PAK1, PTK2B and GSK3B) was increased in TGAC8 vs. WT. These four kinases each phosphorylates various proteins to regulate cellular functions. For example, a previous study observed that in human glioblastoma cell lines, T98G and U87MG cells, the interference of human PDPK1 mRNA by siRNA decreased the phosphorylation level of human BAD protein (S112, S136 and S155) and activated cell death to suppress tumorigenesis[21]. Another study reported that in mouse myoblast cell line, C2C12 cells, PDPK1 protein phosphorylated the mouse ULK1 protein[22]. Increased phosphorylation states of BAD (upregulated at S112, S136 and S155) and ULK1 (upregulated at S450, S521 and S637/638) in TGAC8 may be linked to activated PDPK1.

Different kinases can coordinate to reprogram the complex regulation network in the organism. Consistent with the IPA canonical pathway analysis, the phosphorylation level of 27 proteins (including the three kinases (PDPK1, PAK1 and PTK2B) auto-phosphorylating themselves) were elevated by the three kinases to regulate cardiac stress signaling pathways, including PKA

signaling, ERK/MAPK signaling, cardiac hypertrophy signaling (enhanced), and renin-angiotensin signaling (Figure 1E), to cope with the cardiac stress in the TGAC8. For example, GSK3B is involved in multiple biological processes. PDPK1 phosphorylated GSK3B at S9[23,24] and PTK2B phosphorylated GSK3B at S9 and Y216[25,26] to inhibit the kinase activity of GSK3B. In this phosphoproteome, GSK3B was phosphorylated at multiple sites, including S9, Y216, S219 and S545, and thus GSK3B inhibition was linked to the cardiac adaptation[27,28].

2.3. Downstream functions of the remodeled LV phosphoproteome of TGAC8.

To study the downstream functions of these phosphoproteins, we performed molecular and cellular functions analysis in IPA. The enriched functions were mainly in three categories, i.e., cell viability, protein quality control, and metabolism (Figure 1F and File 2: Sheet5). The functions of cellular assembly and organization, cellular function and maintenance, and cell death and survival were ranked as the top three terms, indicating the important role of the reprogrammed phosphoproteome in improving cell viability in response to the chronic stress of the overexpression of AC8 in the mouse heart.

3. Integrative analyses of transcriptome, proteome and phosphoproteome.

We next integrated changes in PTM (phosphorylation) in TGAC8 vs. WT with genotypic differences in protein translation and in transcription. The circos plot (Figure 3A) illustrates the genotypic differences (TGAC8 vs. WT) in **molecules** identified across the transcriptome, proteome, and phosphoproteome. In addition, the correlation scatter plots (Figure 3B) demonstrated a moderate level of correlation of genotypic differences of molecular changes within phosphoproteome and transcriptome, and a somewhat stronger correlation between genotypic differences of molecular changes within phosphoproteome and proteome (Figure 3C). Concordant and discordant enrichments of canonical pathways differed by genotype among the three omics are shown in Figure 3D. A comparison of genotypic differences within the three omics highlights the importance of protein phosphorylation, and the phosphorylation was **coordinated with and supplemental to** transcription and translation.

Because kinases and phosphatases are the key regulators of phosphorylation, and phosphorylation of transcriptional factors (TFs) are the primary determinant of their activities in transcription, we compared genotypic differences in kinases, phosphatases and TFs within the phosphoproteome and proteome with our previously published genotypic differences in the TGAC8 vs. WT transcriptome[10] (Figure 3E). We identified 196 kinases, 71 phosphatases and 191 TFs in the present phosphoproteome (Figure 3F). The protein phosphorylation status of about one half of these molecules differed significantly (p-value < 0.05) by genotype (Figure 3G), and the protein phosphorylation status of majority of these molecules was increased (Figure 3H-3J). The genotypic differences in the transcription (mRNA expression obtained from RNA-seq) and translation (protein expression obtained from mass spectrometry) of these molecules,

however, differed from those in the phosphoproteome (Figure 3E). Because there were more molecules that were unchanged or reduced in the TGAC8 vs. WT transcriptome or proteome than in the phosphoproteome, it is clear that the changes in protein phosphorylation are of utmost importance in the coordination of transcription, translation and PTM, that underlie the adaptive response of the TGAC8 LV to the marked, chronic increase stress of its intrinsically activated AC-cAMP-PKA-Ca^{2+} signaling. Thus, by utilizing multiple bioinformatic analysis methods, we not only dissected the reprogrammed phosphoproteome and deduced its functions in the TGAC8 mouse LV, but also profiled the coordination of phosphoproteome, transcriptome and proteome.

3.1. Implications of coordinated changes in protein phosphorylation and transcription in TGAC8 vs. WT.

The most likely type of coordination between protein phosphorylation and transcription is related to phosphorylation states of TFs which is determined by kinases and phosphatases activities. Analysis of the remodeled LV transcriptome of TGAC8 in Gene Ontology (GO) analysis using DAVID online software discovered that enrichments of numerous phosphorylation and dephosphorylation related biological processes and molecular functions significantly differed by genotype (Figure 4A), and that the coordinated expression of numerous kinases and phosphatases also differed by genotype (Figure 4B-4C and File 8). Because expression levels of kinases and phosphatases do not denote their activation states, we utilized IPA to predict the genotypic differences in activation states of upstream kinase and phosphatase (regulators of the transcriptome). Intriguingly, 60 kinases were predicted to be upstream regulators of the remodeled LV transcriptome of TGAC8, and the majority of these kinases were predicted to be activated in TGAC8 vs. WT (Figure 4D and File 9). In contrast, many fewer phosphatases were predicted between TGAC8 and WT, and most of these were predicted to be inhibited (Figure 4E and File 9). Thus, the differential genotypic enrichment of phosphorylation status and predicted activation of kinases and phosphatases identified in our post hoc analysis of our previously reported TGAC8 vs. WT transcriptome[10] are linked to the differential genotypic reprogramming of the phosphoproteome discovered in the present study.

We utilized IPA to predict the activation states of upstream transcription regulators on the basis of the remodeled LV transcriptomes and proteomes, and then determined their expression levels in transcriptome, proteome and phosphoproteome (Figure 4F). Because TFs are the main regulators of transcription, and because phosphorylation of TFs usually regulates their activities[29-31], we focused our subsequent analysis on functions of those TFs that were differentially phosphorylated in TGAC8 vs. WT. To confirm the hypothesis that the TGAC8 might exert transcriptional control by TFs phosphorylation, we retrieved all TFs identified in our previous transcriptome and proteome[10] and mapped them to the current phosphoproteome in order to determine their genotypic differences in phosphorylation status. Of the 191 TFs also identified in this phosphoproteome, 92 TFs differed significantly by genotype in phosphorylation status (p-value < 0.05). In agreement with the general upregulated transcription in TGAC8 LV[10], nearly all of the TF that differed by genotype had increased phosphorylation level (Figure 4G

and File 3). The only exception was purine rich element binding protein G (Purg), known to be hyper-phosphorylated in solid tumors[32].

We conducted Kyoto Encyclopedia of Genes and Genomes (KEGG) pathway analysis to further probe the predicted facts of TFs that were generally hyper-phosphorylated in TGAC8 vs. WT. Numerous immunity related pathways, cancer related pathways, and metabolism related pathways were enriched (Figure 4H and File 4). We then utilized IPA for in-depth analysis. Numerous metabolic canonical pathways (glucocorticoid receptor signaling and PPAR signaling), a cancer related canonical pathway (regulation of epithelial-mesenchymal transition pathway), and immunity related canonical pathways (role of JAK1, JAK2 and TYK2 in interferon signaling, IL-9 signaling, JAK/Stat signaling, etc.) were enriched (Figure 4I and File 5: Sheet 1). Intriguingly, the sumoylation pathway was markedly inhibited. Because both sumoylation and phosphorylation are important PTMs in transcriptional regulation[33,34], it is possible that the upregulated protein phosphorylation and inhibited protein sumoylation pathway in TFs coordinately activate transcription and improve immunity in the TGAC8 LV. In addition, cell viability and metabolism in molecular and cellular functions were enriched in TGAC8 vs. WT (Figure 4J and File 5: Sheet 2), consistent with enrichments of afore mentioned KEGG pathways and IPA canonical pathways (Figure 4H and 4I).

Taken together, we have discovered the existence of substantial crosstalk between protein phosphorylation and transcription in the TGAC8 LV: phosphorylation of TFs reprograms immunity and metabolism pathways and functions in the TGAC8 LV, likely serving to maintain cell survival in response to the chronic stress of marked AC8 overexpression.

3.2. Coordinated changes in protein expression and phosphorylation of the remodeled proteome and phosphoproteome of TGAC8.

Having discovered the coordinated changes in the remodeled TGAC8 transcriptome and phosphoproteome (Figure 4A-4E), we next sought to discover the extent to which changes in the remodeled phosphoproteome of the TGAC8 LV were coordinated with changes in its remodeled proteome. Numerous biological processes and molecular functions that were related to phosphorylation and dephosphorylation were enriched in the remodeled TGAC8 LV proteome (Figure 5A), as were numerous kinases and phosphatases (Figure 5B-5C and File 10). Twenty-nine kinases that differed by genotype were predicted to be upstream regulators of the proteome, and most of these were predicted to be activated in TGAC8 vs. WT. Fewer phosphatases than kinases that differed by genotype were identified as upstream regulators of the remodeled TGAC8 LV proteome (Figure 5D-5E and File 11).

One strategy adopted to probe deeper into the coordinated changes in the proteome and phosphoproteome of the TGAC8 LV was to normalize the phosphoproteome to the total proteome (in other words, to divide the phosphorylation expression by protein expression) (File 1: sheet4). Of the 3927 phosphoproteins identified in our mouse LV samples, 2164 were identified in both the proteome and phosphoproteome, and these were focused for subsequent analyses.

After normalization, WT and TGAC8 samples manifested clear genotypic differences in PCA analysis (Figure 5G), and phosphorylation status of numerous proteins normalized to the protein expression level still differed by genotype without cutoff (Figure 5H) and with cutoff (-log(p-value) > 1.3 and absolute(log2(TG/WT)) ≥ 0.4) (Figure 5I). Even after normalizing the phosphorylation level to the protein expression level, the enrichments of canonical pathways in TGAC8 were quite consistent with those of unnormalized phosphoproteome (Figure 5J and File 6). Cardiac hypertrophy signaling (enhanced) and cardiac hypertrophy signaling took the top two places, emphasizing the important role of phosphorylation in the regulation of cardiac functions in response to chronic stress when coordinated with changes in the total proteome.

Many important stress-response signaling pathways were enriched from phosphoproteome, e.g., PKA signaling, ERK/MAPK signaling, insulin receptor signaling, and PI3K/AKT signaling (Figure 6A). Three of these pathways, PI3K/AKT, ERK/MAPK and ubiquitin labeling, were also markedly enriched in our previous analysis on total proteome in TGAC8 LV[35]. By integrating and comparing the enrichments from transcriptome, proteome and phosphoproteome, we were able to identify the three signaling pathways in the TGAC8 LV, PI3K/AKT, ERK/MAPK and ubiquitin labeling, that were regulated concordantly in transcription, translation, and PTM (phosphorylation) (Figure 6B). PI3K/AKT and ERK/MAPK signaling pathways are not only enriched but also activated in TGAC8. We verified the phosphorylation and activation of PI3K/AKT (Figure 7A-7B) and ERK/MAPK (Figure 7C) signaling pathways via WB. Their activations are crucial for the increase in protein synthesis and cell survival in the TGAC8 LV[35]. Protein ubiquitination is an important process in protein degradation, which is also increased in TGAC8 LV[35], but the activity of this pathways could not be predicted on the basis of present knowledge base of IPA. Therefore, we conducted wet lab experiments. The rate of protein synthesis was 40% higher in TGAC8 than in WT (Figure 7D). Proteosome activity, which helps to limit the increased protein load of TGAC8 hearts, was also increased in TGAC8 vs. WT (Figure 7E). Therefore, although there was a significant increase in the amount of soluble misfolded proteins in the TGAC8 LV (Figure 7F), insoluble protein aggregates did not accumulate within the TGAC8 LV (Figure 7G). Our experiment results confirmed the enhanced protein synthesis and degradation to improve the proteasome.

We next sought to identify which molecules linked to PI3K/AKT signaling differed in TGAC8 vs. WT. Among the significantly changed upstream molecules, the majority were upregulated. AKT, a central molecule in the pathway, was also increased in proteome and phosphoproteome (Figure 6C). By searching and mapping the substrates of AKT, we unraveled that the phosphorylation levels of AKT peptide substrates were mostly elevated in TGAC8 vs. WT (Figure 6D and Supplementary Figure 3). Therefore, the downstream effects and functions of AKT signaling were activated in TGAC8 LV: (1) upregulating GSK3 to improve energy metabolism; (2) activating mTOR pathway to increase protein synthesis and cell growth; (3) promoting NF-κB mediated transcription; (4) upregulating BAD and eNOS only at phosphorylational level to enhance cell survival and cardiovascular functions. In summary, to

adapt the heart to stress for improved survival, the TGAC8 upregulates the protein phosphorylation to reprogram the cardiac LV phosphoproteome.

4. Discordant regulation of the phosphoproteome and proteome in TGAC8 LV.

Among the 443 proteins that differed by genotype in both protein phosphorylation and protein expression levels, 33 were changed discordantly at the two levels (in opposite directions, i.e., upregulated in proteome but downregulated in phosphoproteome, or vice versa) (Figure 8A and File 7: Sheet 1). We uploaded the 33 discordant proteins into STRING online software for functional analyses. The GO_CC (Cellular Component) analysis resulted in many **mitochondrial components**, indicating the involvement of phosphorylated proteins in mitochondria (Figure 8B and File 7: Sheet 2). Reactome pathway analysis showed that in addition to mitochondria, metabolic pathways were enriched significantly in TGAC8 (Figure 8C and File 7: Sheet 3). Mitochondria are the hub of metabolism and multiple metabolic processes are executed in mitochondria. Consistently, both metabolism and mitochondria related processes were ranked the top processes in GO_BP (Biological Process) analysis (Figure 8D and File 7: Sheet 4). Therefore, the discordant part between total proteome and phosphoproteome indicated that the phosphorylation plays a critical role in the regulation of mitochondria and metabolism in the TGAC8, distinct from its role in regulation at the translational level.

5. Deduced schematic of coordination of phosphoproteome with transcriptome and proteome in TGAC8 mouse LV.

A deduced schematic integration of the remodeled phosphoproteome, proteome and transcriptome of the TGAC8 LV is shown in Figure 9. The TGAC8 mouse first induces a PKA dependent phosphorylation via AC8-cAMP-PKA axis. Many cytoplasmic proteins including TFs are thus phosphorylated and then transported into the nucleus where TFs recognize and bind to the promoters to activate the transcription of more regulatory factors, including kinases, phosphatases, and TFs. The activation states of these factors are changed upon phosphorylated in cytosol, thereby activating additional kinases-controlled phosphorylation cascades and reprogramming the cardiac phosphoproteome comprehensively.

Discussion

Our prior study[35] investigated the adaptive mechanisms that emerge in the TGAC8 heart to marked chronic stress of increased AC8-cAMP-PKA-Ca^{2+} signaling. In that study, a large number of proteins differed in TGAC8 vs. WT. The TGAC8 induced a chronic cardiac exercise phenotype in the heart, i.e., an increase in heart rate and contractility. These functional changes were accompanied by an increased cardiac biomass and energy demand. Multiple signaling

pathways, related to nutrient sensing, energy production, cardiac cellular stress, cardiac stress response, growth factor signaling, and cell proliferation, were identified as downstream mediating the effect of the activated AC8-cAMP-PKA-Ca^{2+} signaling in the TGAC8 LV.

Our goals here were to determine which proteins in TGAC8 LV differed in expression and phosphorylation status compared to WT, and which kinases/phosphatases play a role in these altered phosphorylation statuses in the TGAC8. By the utilization of TMT-labeling MS, we obtained 12963 phosphopeptides and 3646 phosphoproteins, and observed the general upregulation of phosphorylation. We observed the enrichments of phosphorylation, upregulated expression of kinases, and predicted activation of upstream kinases. We made use of phosphoproteome complementary to transcriptome and proteome to expand our understanding of the regulatory mechanism how the TGAC8 adapts to chronic stress of activated AC8-cAMP-PKA-Ca^{2+} signaling. This approach enabled us to appreciate how changes in the transcription, translation and PTM of proteins in the TGAC8 LV may singly or coordinately enable the TGAC8 to endure the chronic AC8-induced stress (Figure 9).

First, the TGAC8 induced a PKA dependent phosphorylation via the AC8-cAMP-PKA axis (typical substrate motif of PKA dependent phosphorylation). Most of previous studies only focused on PKA phosphorylated targets as downstream effects of activated AC8. For example, AC8 induced cAMP activates PKA to increase the phosphorylation of many key proteins in cardiovascular system, e.g., ryanodine-receptor-type 2 (RyR2), L-type Ca^{2+} channels (LTCC), phospholamban (PLN or PLB), etc[36]. In this research, we identified 29 phosphosites on RyR2, 15 phosphosites on LTCC alpha 1 and beta 2, and 2 phosphosites (S16 and T17) on PLN, SERCA2 and the majority of them were increased in phosphorylation statuses in the TGAC8 LV (File 1: Sheet 1). It is worth noting that PLN is phosphorylated on S16 by PKA whereas on T17 by Ca^{2+}-calmodulin-dependent protein kinase (CaMKII)[37].

After the activation of phosphorylation cascade, many cytoplasmic proteins including TFs were thus phosphorylated and then transported into the nucleus where TFs recognize and bind to the promoters to activate transcription. For example, Figure 4 F and 4G showed that many transcriptional regulators were phosphorylated in TGAC8 vs. WT. The phosphorylation of STAT1[38,39], STAT3[39], HTT[40] and CREB1[41] is associated with the activation of their transcriptional activities. The elevated TFs phosphorylation and possibly activated transcription were consistent with the general increase in transcriptome[35]. The hyper-phosphorylated TFs might contribute to the improved immunity, metabolism and cell viability in TGAC8 (Figure 4H-4I). For example, STAT family proteins are transcription activators, and their phosphorylation is involved in inflammation and immune response[42,43]. The present study identified increased phosphorylation levels in S727 on STAT1 and S726/S727 on STAT3 (File 1: Sheet 1), in line with our previous report which identified hyper-phosphorylation of components within inflammation and immune response signaling pathways such as JAK/STAT and JNK pathways[10].

Upon the activation of RNA transcription, numerous molecules, including kinases, phosphatases, and TFs, were transcribed more in TGAC8 than WT, thereby, activating other kinases-controlled phosphorylation cascades in addition to PKA. The additional kinases and phosphorylation cascades could also be directly activated by the overexpression of AC8 in another manner to be determined. In this study, with the three datasets, IPA predicted many other kinase-substrate reactions in addition to PKA. PDPK1, PAK1 and PTK2B were the three most consistent kinases. In the context of the overexpression of AC8, these three kinases could be activated to phosphorylate multiple proteins to activate PKA pathway (positive feedback) and MAPK/ERK pathway (also known as Ras-Raf-MEK-ERK pathway) to maintain heart health (Figure 1E and Supplementary Figure 2). Previously, we showed their western blot results that MAPK/ERK pathway were activated due to increased protein expression of p21 Ras and the elevated phosphorylation levels of c-Raf, MEK1/2 and ERK1/2 as well as their increased ratios of phosphorylation to protein expression[10]. In the present study, S233 and S621/S641 were hyper-phosphorylated in TGAC8 (File 1: Sheet 1). Importantly, the multifunctional molecule, GSK3B, was the downstream of PDPK1 and PTK2B in the integrated regulation network. GSK3B is involved in metabolism and cardiac hypertrophy[44,45]. Interestingly, AC8 is required for glucose homeostasis and hypothalamic adaptation to high-fat diet[46]. The phosphorylation of GSK3B is also a critical mediator in convergence of cardioprotection signaling[27,28]. We previously detected the increase in the protein expression of GSK3B[10] and here identified the hyper-phosphorylated S9 on GSK3B (File 1: Sheet 1). The bioinformatic analysis strategy here revealed a larger kinase-substrate network important in the remodeling of the TGAC8 heart. We plan to validate these kinase-substrate reactions in follow-up studies and provide the reliable mechanism in cardiovascular research.

Taken together, the TGAC8 upregulates phosphorylation to reprogram the heart. Based on results in this study combined with our recently published work on TGAC8 LV[10], we generated a comprehensive circuitry (Figure 10). Navigating this figure "by the numbers": marked, chronic, cardiac specific overexpression of AC8 (1) chronically increases cAMP (2) and PKA-Ca^{2+} signaling (3), resulting, not only in an incessantly increased cardiac performance, due to elevated heart rate and LV contractility (4), but also activation of growth factor signaling pathways (5), leading to increase in energy demand due to increased transcription and increased amino acid, nucleotide, protein, lipid and lipoprotein synthesis, increased protein quality control, including proteosome activity, autophagy, mitophagy, cytokine signaling and inflammation (6). Chronic high level of AC8 activation elicits numerous stress responses (8) including increased nutrient sensing with increase AMPK signaling (10A), increased ROS scavenging, protection against cell death, and also induction of signaling to minimize the impact of AC-PKA signaling (10B). Shifts in energy production and utilization to deal with the marked energy demands of the TGAC8 heart (10, 12) include: enhancement of glucose metabolism is pronounced (11, 13), whilst utilization of fatty acids to produce energy is reduced (11) but an increase in glucose catabolism (10, 11) is accompanied by an increased anabolism (12), supported by increased aerobic glycolysis (11,13); increased utilization of the pentose phosphate shunt (5, 13) supports increased

amino acid, nucleotide, protein and lipoprotein synthesis induced by growth factor signaling (5), resulting in an increase in LV biomass (14). This adaptive profile balances energy requirements necessary for an incessant marked increase in cardiac performance (4), for increased RNA transcription, protein translation and quality control required for cardiac growth (14), and for other biological processes within the LV myocardium (6). This pattern of consilient adaptations (6-15) sustains an incessant increase in cardiac performance while conferring cardio-protection to the TGAC8 heart.

In addition to the fascinating adaptive mechanisms in the TGAC8 LV discussed above, the present research also raised some interesting open-mind questions, such as cardiac hypertrophy signaling and sumoylation pathway enriched here.

Although the cardiac β-AR signaling is desensitized in many pathological conditions, like aging, so as to despair the cardiovascular system functions, cAMP bioavailability could maintain cardiac functions in the aged heart. Based on this, the overexpression of AC8 in heart was regarded as a potential therapeutic way to increase the bioavailability of cardiac cAMP independent of β-AR stimulation to improve cardiac functions[7]. Unexpectedly, the cardiac-specific chronic activation of the cAMP pathway (overexpressing β1- AR, β2-AR, Gas, PKA, I-I, etc.) that enhances cardiac functions in young animals induces progressive cardiomyopathy and premature death during aging[47]. Consistently, in the present research, although the enriched cardiac hypertrophy signaling (enhanced) was not accompanied with the markable hypertrophy phenotype in young male TGAC8 mice, it indicated a cardiac remodeling that could lead to hypertrophy if accompanied with additional stresses, like aging. This assumption was supported by another research on the TGAC8 mouse which reported early alterations of myocardial structure, i.e., cardiomyocyte hypertrophy and endocardial fibrosis, in twelve-month old TGAC8 mice compared with their WT littermates[48]. Therefore, our established bioinformatic analysis strategy is a novel paradigm in **predicting** progressive cardiomyopathy and premature death using early reprograming of omics in young age. More importantly, the mechanisms discovered here in the young adult TGAC8 mice could be utilized in maintaining cardiac health in older TGAC8 mice.

Interestingly, more and more PTMs have been discovered nowadays and they often occur at the same time or on the same protein to carry important biological processes coordinately[49,50]. For example, in rat hearts subjected to ischemia, lysine acetylation interferes with activities of protein kinases to increase proximal dephosphorylation, which is involved in the regulation of cell survival or death[51]. In the present research, sumoylation pathway was inhibited along with the upregulated phosphorylation (Figure 4I), indicating the cross-talk between these two PTMs in the mouse heart. In human cell-lines, the switch from phosphorylation to sumoylation could repress the Raf/MEK/ERK signaling to improve the immunity, resulting in the declined infection of influenza A virus[52]. In human HEK293 cells, the coordinated phosphorylation and sumoylation can also control MEF2 transcriptional activity[53]. However, the competition of phosphorylation and sumoylation in cardiomyocytes was unclear. In this research, we observed

the upregulated phosphorylation and inhibited sumoylation pathway enriched from TFs in the TGAC8 mouse LV. The regulated PTMs were speculated to be involved in the increased transcription and improved immunity. To validate the effect on sumoylation by elevated phosphorylation in our next studies, we could perform WB with the antibody against pan-sumoylation to detect the general sumoylation change in the TGAC8 LV. In addition, we could detect the sumoylation changes after mimicry upregulation or downregulation of phosphorylation using activators or inhibitors in primary cardiomyocytes to prove the interplay between phosphorylation and sumoylation in cardiomyocytes.

In summary, the reprogrammed phosphoproteome activated stress response signaling pathways to defend against cardiac stress in young mice, improve cell viability and suppress cell death. On one hand, the reprogramed phosphoproteome enhances transcription to improve the immunity and metabolism; on the other hand, it coordinates with the proteome to improve mitochondrial functions and metabolism. Finally, although we revealed the coordination of regulation at different levels, which provides a roadmap to guide the integration of transcription, translation and PTM, our results set the stage for additional studies in this remarkable TGAC8 model: What kinases are specifically involved in the PTM identified here? How are these phosphorylated proteins specifically distributed in subcellular locations? The present study focuses on a comprehensive in silico analysis of functionally coherent and data-driven transcription, translation, and post-translation patterns that were well translated in the contribution to AC8-overexpression cardiac outcomes, while further investigation is warranted to see whether the hub pathway/function predictions via gene sets, phosphopeptides, and phosphoproteins could be used as biomarkers or impact the diagnostic specificity for transgenic AC8 cardiac health and pathology.

Acknowledgements

We thank all members in Laboratory of Cardiovascular Science, National Institute on Aging, National Institutes of Health, for technical assistance and discussion. This work utilized the computational resources of the NIH HPC Biowulf cluster (http://hpc.nih.gov).

Sources of Funding

Intramural Research Program at National Institute on Aging, National Institutes of Health.

Disclosures

None.

References

1 Halls, M. L. & Cooper, D. M. F. Adenylyl cyclase signalling complexes - Pharmacological challenges and opportunities. *Pharmacol Ther* **172**, 171-180 (2017). https://doi.org:10.1016/j.pharmthera.2017.01.001

2 Dessauer, C. W. *et al.* International Union of Basic and Clinical Pharmacology. CI. Structures and Small Molecule Modulators of Mammalian Adenylyl Cyclases. *Pharmacological reviews* **69**, 93-139 (2017). https://doi.org:10.1124/pr.116.013078

3 Willoughby, D. *et al.* A key phosphorylation site in AC8 mediates regulation of Ca(2+)-dependent cAMP dynamics by an AC8-AKAP79-PKA signalling complex. *J Cell Sci* **125**, 5850-5859 (2012). https://doi.org:10.1242/jcs.111427

4 Sadana, R. & Dessauer, C. W. Physiological roles for G protein-regulated adenylyl cyclase isoforms: insights from knockout and overexpression studies. *Neuro-Signals* **17**, 5-22 (2009). https://doi.org:10.1159/000166277

5 Georget, M. *et al.* Augmentation of cardiac contractility with no change in L-type Ca2+ current in transgenic mice with a cardiac-directed expression of the human adenylyl cyclase type 8 (AC8). *Faseb j* **16**, 1636-1638 (2002). https://doi.org:10.1096/fj.02-0292fje

6 Ferguson, G. D. & Storm, D. R. Why calcium-stimulated adenylyl cyclases? *Physiology (Bethesda, Md.)* **19**, 271-276 (2004). https://doi.org:10.1152/physiol.00010.2004

7 Lipskaia, L. *et al.* Enhanced cardiac function in transgenic mice expressing a Ca(2+)-stimulated adenylyl cyclase. *Circ. Res.* **86**, 795-801 (2000). https://doi.org:10.1161/01.res.86.7.795

8 Esposito, G. *et al.* Increased myocardial contractility and enhanced exercise function in transgenic mice overexpressing either adenylyl cyclase 5 or 8. *Basic Res Cardiol* **103**, 22-30 (2008). https://doi.org:10.1007/s00395-007-0688-6

9 Moen, J. M. *et al.* Overexpression of a Neuronal Type Adenylyl Cyclase (Type 8) in Sinoatrial Node Markedly Impacts Heart Rate and Rhythm. *Front Neurosci* **13**, 615 (2019). https://doi.org:10.3389/fnins.2019.00615

10 Tarasov, K. V. *et al.* A remarkable adaptive paradigm of heart performance and protection emerges in response to the constitutive challenge of marked cardiac-specific overexpression of adenylyl cyclase type 8. *eLife* **11**, e80949 (2022). https://doi.org:10.7554/eLife.80949

11 Qu, J.-H. *et al.* Proteomic Landscape and Deduced Functions of the Cardiac 14-3-3 Protein Interactome. *Cells* **11**, 3496 (2022). https://doi.org:10.3390/cells11213496

12 Consortium, T. U. UniProt: a worldwide hub of protein knowledge. *Nucleic Acids Res.* **47**, D506-D515 (2018). https://doi.org:10.1093/nar/gky1049

13 Crooks, G. E., Hon, G., Chandonia, J. M. & Brenner, S. E. WebLogo: a sequence logo generator. *Genome research* **14**, 1188-1190 (2004). https://doi.org:10.1101/gr.849004

14 Colaert, N., Helsens, K., Martens, L., Vandekerckhove, J. & Gevaert, K. Improved visualization of protein consensus sequences by iceLogo. *Nat Methods* **6**, 786-787 (2009). https://doi.org:10.1038/nmeth1109-786

15 Mitaku, S., Hirokawa, T. & Tsuji, T. Amphiphilicity index of polar amino acids as an aid in the characterization of amino acid preference at membrane-water interfaces. *Bioinformatics* **18**, 608-616 (2002). https://doi.org:10.1093/bioinformatics/18.4.608

16 Takahashi, S. & Mendelsohn, M. E. Synergistic activation of endothelial nitric-oxide synthase (eNOS) by HSP90 and Akt: calcium-independent eNOS activation involves formation of an HSP90-Akt-CaM-bound eNOS complex. *The Journal of biological chemistry* **278**, 30821-30827 (2003). https://doi.org:10.1074/jbc.M304471200

664 17 Lim, G., Venetucci, L., Eisner, D. A. & Casadei, B. Does nitric oxide modulate cardiac ryanodine
665 receptor function? Implications for excitation-contraction coupling. *Cardiovasc Res* **77**, 256-264
666 (2008). https://doi.org:10.1093/cvr/cvm012
667 18 Meissner, G. in *Structure and Function of Calcium Release Channels Current Topics in*
668 *Membranes* 91-113 (2010).
669 19 Hunzicker-Dunn, M. E. *et al.* PKA and GAB2 play central roles in the FSH signaling pathway to
670 PI3K and AKT in ovarian granulosa cells. *Proceedings of the National Academy of Sciences of the*
671 *United States of America* **109**, E2979-2988 (2012). https://doi.org:10.1073/pnas.1205661109
672 20 Bellis, A. *et al.* Cross-talk between PKA and Akt protects endothelial cells from apoptosis in the
673 late ischemic preconditioning. *Arterioscler Thromb Vasc Biol* **29**, 1207-1212 (2009).
674 https://doi.org:10.1161/atvbaha.109.184135
675 21 Desai, S., Pillai, P., Win-Piazza, H. & Acevedo-Duncan, M. PKC-iota promotes glioblastoma cell
676 survival by phosphorylating and inhibiting BAD through a phosphatidylinositol 3-kinase pathway.
677 *Biochim Biophys Acta* **1813**, 1190-1197 (2011). https://doi.org:10.1016/j.bbamcr.2011.03.007
678 22 Li, Y. *et al.* microRNA-378 promotes autophagy and inhibits apoptosis in skeletal muscle.
679 *Proceedings of the National Academy of Sciences of the United States of America* **115**, E10849-
680 e10858 (2018). https://doi.org:10.1073/pnas.1803377115
681 23 Chen, X. *et al.* PDK1 regulates platelet activation and arterial thrombosis. *Blood* **121**, 3718-3726
682 (2013). https://doi.org:10.1182/blood-2012-10-461897
683 24 Ericson, K. *et al.* Genetic inactivation of AKT1, AKT2, and PDPK1 in human colorectal cancer cells
684 clarifies their roles in tumor growth regulation. *Proceedings of the National Academy of Sciences*
685 *of the United States of America* **107**, 2598-2603 (2010).
686 https://doi.org:10.1073/pnas.0914018107
687 25 Hartigan, J. A., Xiong, W. C. & Johnson, G. V. Glycogen synthase kinase 3beta is tyrosine
688 phosphorylated by PYK2. *Biochemical and biophysical research communications* **284**, 485-489
689 (2001). https://doi.org:10.1006/bbrc.2001.4986
690 26 Tsai, C. C. *et al.* Glycogen synthase kinase-3beta facilitates IFN-gamma-induced STAT1 activation
691 by regulating Src homology-2 domain-containing phosphatase 2. *J Immunol* **183**, 856-864 (2009).
692 https://doi.org:10.4049/jimmunol.0804033
693 27 Juhaszova, M. *et al.* Glycogen synthase kinase-3beta mediates convergence of protection
694 signaling to inhibit the mitochondrial permeability transition pore. *The Journal of clinical*
695 *investigation* **113**, 1535-1549 (2004). https://doi.org:10.1172/JCI19906
696 28 Juhaszova, M. *et al.* Role of glycogen synthase kinase-3beta in cardioprotection. *Circ. Res.* **104**,
697 1240-1252 (2009). https://doi.org:10.1161/CIRCRESAHA.109.197996
698 29 Bohmann, D. Transcription factor phosphorylation: a link between signal transduction and the
699 regulation of gene expression. *Cancer cells (Cold Spring Harbor, N.Y. : 1989)* **2**, 337-344 (1990).
700 30 Weigel, N. L. & Moore, N. L. Steroid receptor phosphorylation: a key modulator of multiple
701 receptor functions. *Molecular endocrinology (Baltimore, Md.)* **21**, 2311-2319 (2007).
702 https://doi.org:10.1210/me.2007-0101
703 31 Mayr, B. & Montminy, M. Transcriptional regulation by the phosphorylation-dependent factor
704 CREB. *Nature reviews. Molecular cell biology* **2**, 599-609 (2001).
705 https://doi.org:10.1038/35085068
706 32 Zanivan, S. *et al.* Solid tumor proteome and phosphoproteome analysis by high resolution mass
707 spectrometry. *J Proteome Res* **7**, 5314-5326 (2008). https://doi.org:10.1021/pr800599n
708 33 Tomanov, K. *et al.* Sumoylation and phosphorylation: hidden and overt links. *Journal of*
709 *Experimental Botany* **69**, 4583-4590 (2018). https://doi.org:10.1093/jxb/ery167

710 34 Khan, M. *et al.* Interplay between phosphorylation and SUMOylation events determines CESTA
711 protein fate in brassinosteroid signalling. *Nat Commun* **5**, 4687 (2014).
712 https://doi.org:10.1038/ncomms5687
713 35 Tarasov, K. V. *et al.* A Remarkable Adaptive Paradigm Of Heart Performance And Protection
714 Emerges In Response To The Constitutive Challenge of Marked Cardiac-Specific Overexpression
715 Of Adenylyl Cyclase Type 8. *bioRxiv*, 2022.2005.2020.491883 (2022).
716 https://doi.org:10.1101/2022.05.20.491883
717 36 Guellich, A., Mehel, H. & Fischmeister, R. Cyclic AMP synthesis and hydrolysis in the normal and
718 failing heart. *Pflugers Arch* **466**, 1163-1175 (2014). https://doi.org:10.1007/s00424-014-1515-1
719 37 Wegener, A. D., Simmerman, H. K., Lindemann, J. P. & Jones, L. R. Phospholamban
720 phosphorylation in intact ventricles. Phosphorylation of serine 16 and threonine 17 in response
721 to beta-adrenergic stimulation. *The Journal of biological chemistry* **264**, 11468-11474 (1989).
722 38 Pilz, A. *et al.* Phosphorylation of the Stat1 transactivating domain is required for the response to
723 type I interferons. *EMBO reports* **4**, 368-373 (2003). https://doi.org:10.1038/sj.embor.embor802
724 39 Wen, Z., Zhong, Z. & Darnell, J. E., Jr. Maximal activation of transcription by Stat1 and Stat3
725 requires both tyrosine and serine phosphorylation. *Cell* **82**, 241-250 (1995).
726 https://doi.org:10.1016/0092-8674(95)90311-9
727 40 Kumar, A., Vaish, M. & Ratan, R. R. Transcriptional dysregulation in Huntington's disease: a
728 failure of adaptive transcriptional homeostasis. *Drug Discov. Today* **19**, 956-962 (2014).
729 https://doi.org:10.1016/j.drudis.2014.03.016
730 41 Wang, H., Xu, J., Lazarovici, P., Quirion, R. & Zheng, W. cAMP Response Element-Binding Protein
731 (CREB): A Possible Signaling Molecule Link in the Pathophysiology of Schizophrenia. *Frontiers in*
732 *molecular neuroscience* **11**, 255-255 (2018). https://doi.org:10.3389/fnmol.2018.00255
733 42 Seif, F. *et al.* The role of JAK-STAT signaling pathway and its regulators in the fate of T helper
734 cells. *Cell Communication and Signaling* **15**, 23 (2017). https://doi.org:10.1186/s12964-017-
735 0177-y
736 43 Decker, T. & Kovarik, P. Serine phosphorylation of STATs. *Oncogene* **19**, 2628-2637 (2000).
737 https://doi.org:10.1038/sj.onc.1203481
738 44 Beurel, E., Grieco, S. F. & Jope, R. S. Glycogen synthase kinase-3 (GSK3): regulation, actions, and
739 diseases. *Pharmacol Ther* **148**, 114-131 (2015).
740 https://doi.org:10.1016/j.pharmthera.2014.11.016
741 45 Lal, H., Ahmad, F., Woodgett, J. & Force, T. The GSK-3 family as therapeutic target for myocardial
742 diseases. *Circ Res* **116**, 138-149 (2015). https://doi.org:10.1161/circresaha.116.303613
743 46 Raoux, M. *et al.* Multilevel control of glucose homeostasis by adenylyl cyclase 8. *Diabetologia* **58**,
744 749-757 (2015). https://doi.org:10.1007/s00125-014-3445-z
745 47 El-Armouche, A. & Eschenhagen, T. Beta-adrenergic stimulation and myocardial function in the
746 failing heart. *Heart failure reviews* **14**, 225-241 (2009). https://doi.org:10.1007/s10741-008-
747 9132-8
748 48 Mougenot, N. *et al.* Cardiac adenylyl cyclase overexpression precipitates and aggravates age-
749 related myocardial dysfunction. *Cardiovascular research* **115**, 1778-1790 (2019).
750 https://doi.org:10.1093/cvr/cvy306
751 49 Beltrao, P., Bork, P., Krogan, N. J. & van Noort, V. Evolution and functional cross-talk of protein
752 post-translational modifications. *Molecular systems biology* **9**, 714 (2013).
753 https://doi.org:10.1002/msb.201304521
754 50 Venne, A. S., Kollipara, L. & Zahedi, R. P. The next level of complexity: crosstalk of
755 posttranslational modifications. *Proteomics* **14**, 513-524 (2014).
756 https://doi.org:10.1002/pmic.201300344

51 Parker, B. L. *et al.* Structural basis for phosphorylation and lysine acetylation cross-talk in a kinase motif associated with myocardial ischemia and cardioprotection. *The Journal of biological chemistry* **289**, 25890-25906 (2014). https://doi.org:10.1074/jbc.M114.556035

52 Wang, C. *et al.* HA Triggers the Switch from MEK1 SUMOylation to Phosphorylation of the ERK Pathway in Influenza A Virus-Infected Cells and Facilitates Its Infection. *Frontiers in cellular and infection microbiology* **7**, 27 (2017). https://doi.org:10.3389/fcimb.2017.00027

53 Grégoire, S. *et al.* Control of MEF2 transcriptional activity by coordinated phosphorylation and sumoylation. *The Journal of biological chemistry* **281**, 4423-4433 (2006). https://doi.org:10.1074/jbc.M509471200

Figure Legends

Figure 1. TGAC8 reprograms the LV phosphorylation state. A. PCA plot of phosphoproteome in TGAC8 vs. WT LVs. **B**. Heatmap of scaled expressions of phosphorylated proteins. **C**. Volcano plot of phosphoproteome. Red dots represent upregulated phosphoproteins with -log10(p-value) > 1.3 and log2(fold change) ≥ 0.4; blue dots represent downregulated phosphoproteins with -log10(p-value) > 1.3 and log2(fold change) ≤ -0.4; grey dots represent nonsignificantly regulated phosphoproteins with -log10(p-value) ≤ 1.3 or absolute(log2(fold change)) < 0.4. **D**. Top 21 canonical pathways enriched from phosphoproteome. Orange and blue bars represent activated and inhibited pathways respectively. The darker the color is, the greater the absolute(z-score) is, and the more significantly enriched the pathway is. **E**. Regulatory pathway from upstream kinases. Three dots in the center represent the predicted upstream kinases. Surrounding dots represent identified phosphoproteins differentially regulated in phosphoproteome. Terms on the bottom represent canonical pathways in which the phosphoproteins are involved. Meanings of colors refer to the box of prediction legend besides the graph. **F**. Enriched molecular and cellular functions from the phosphoproteome. They are related to three categories, including cell viability, protein quality control, and metabolism.

Figure 2. Characteristics of upregulated phosphopeptides. A. Composition of phosphosites that reside on the upregulated phosphopeptides. **B**. Sequence logo diagrams of upregulated phosphopeptides centered on the phosphosites and flanked by 6 amino acids on the N and C termini respectively using WebLogo online software. Colors of amino acids represent different chemical properties. **C**. Test the amphiphilicity feature of the upregulated phosphopeptides using iceLogo online software and referring to a published work by Mitaku and colleagues in 2002.

Figure 3. Integrative analysis of transcriptome, proteome and phosphoproteome. A. Circos plot of gene expression at different levels from transcription, to protein, and to phosphorylation. Bars in each layer of circle represent changes of significantly regulated molecules (q-value or p-value < 0.05) in transcriptome, total proteome, and unnormalized phosphoproteome. Bar height, color and direction represent log2(fold change). Red and upward indicate upregulation, and blue and downward indicate downregulation. **B-C**. Scatter plots of correlation between phosphoproteome and transcriptome (**B**) or

total proteome (**C**). **D**. Comparison of canonical pathway enrichments from the transcriptome, total proteome, and phosphoproteome. Enrichment z-scores were calculated in IPA, and were scaled to generate heatmap in R language. **E**. Integrative graph of expression of all phosphoproteins and selected types of molecules. Bar plot on the bottom displays expression of all significantly changed (p-value < 0.05) phosphoproteins in unnormalized phosphoproteome. Y-axis denotes log2(fold change), and x-axis denotes each molecule ranked by log2(fold change). Bars were colored by -log10(p-value). Stick plots on the top display kinases, phosphatases and transcription factors (TFs) selected from the bottom bar plot and their changes in transcriptome (RNA), total proteome (pro), and normalized phosphoproteome (norm). From top to bottom: each large block denotes the changes of certain types of molecules (from kinases to phosphatases, to TFs). In each block, the three rows from top to bottom indicate the changes in transcriptome, total proteome, and normalized phosphoproteome. Each stick represents a molecule and color represents the change: red: (p-value or q-value < 0.05) and log2FC > 0; blue: (p-value or q-value < 0.05) and log2FC < 0; black: (p-value or q-value ≥ 0.05) or log2FC = 0; grey: unidentified in one of the omics. Their locations are matched to those in the bottom bar plot. **F-J**. Pie plots of composition of phosphoproteins in the unnormalized phosphoproteome. Regardless of p-value, numbers of four types of proteins, including kinases, phosphatases, TFs and others, are displayed in **F**. After filtration with cutoff p-value < 0.05, numbers of those types of proteins are displayed in **G**. Extracted from G, numbers of upregulated and downregulated kinases (**H**), phosphatases (**I**) and TFs (**J**) are displayed.

Figure 4. Coordination of phosphoproteome and transcriptome. A. GO term enrichments of biological processes and molecular functions about phosphorylation and dephosphorylation from transcriptome. **B**-**C**. Changes of kinases (**B**) and phosphatases (**C**) whose q-values are less than 0.05 in transcriptome. **D**-**E**. States of upstream kinases (**D**) and phosphatases (**E**) predicted based on transcriptome. Z-scores were calculated in IPA. Positive and negative z-scores indicate activated and inhibited states respectively. The larger absolute values of z-score indicate more activated or inhibited states. **F**. Heatmap of predicted upstream transcription regulators (left) and their changes in different omics datasets (right). Left: Fill color represent activation z-scores in transcriptome and total proteome. Red and blue indicate activated and inhibited states respectively. Molecules are ranked by z-scores in transcriptome. Right: Fill color represent changes in transcriptome, total proteome, unnormalized phosphoproteome, and normalized phosphoproteome: orange: (p-value or q-value < 0.05) and log2FC > 0; yellow: (p-value or q-value ≥ 0.05) and log2FC > 0; green: (p-value or q-value < 0.05) and log2FC < 0; light blue: (p-value or q-value ≥ 0.05) and log2FC < 0; grey: unidentified in one of the omics. **G**. Changes of differentially regulated TFs with p-value < 0.05 in the unnormalized phosphoproteome. **H**. KEGG pathway enrichments of the differentially regulated TFs. They are in four primary categories: cancer, immunity, metabolism and others. **I**. Top 20 canonical pathways enriched from the phosphoproteome using IPA. The darker the color is, the greater the absolute(z-score) is, and the more significantly enriched the pathway is. **J**. Enriched molecular and cellular functions from the phosphoproteome using IPA. They are in two primary categories: cell viability and metabolism.

Figure 5. Analysis of normalized phosphoproteome. A. GO term enrichments of biological processes and molecular functions about phosphorylation and dephosphorylation from the present proteome. **B**-**C**.

Changes of kinases (**B**) and phosphatases (**C**) whose q-values are less than 0.05 in previous proteome. **D-E**. States of upstream kinases (**D**) and phosphatases (**E**) predicted based on the present proteome. Z-scores were calculated in IPA. Positive and negative z-scores indicate activated and inhibited states respectively. The larger absolute values of z-score indicate more activated or inhibited states. **F**. Venn plot of new total proteome and unnormalized phosphoproteome that were conducted concurrently in the same platform. **G**. PCA plot of phosphoproteome normalized to total proteome. **H**. Heatmap of expressions of phosphoproteins normalized to total proteins. **I**. Volcano plot of normalized phosphoproteome. Red dots represent upregulated phosphoproteins with -log10(p-value) > 1.3 and log2(fold change) ≥ 0.4; blue dots represent downregulated phosphoproteins with -log10(p-value) > 1.3 and log2(fold change) ≤ -0.4; grey dots represent nonsignificantly regulated phosphoproteins with -log10(p-value) ≤ 1.3 or absolute(log2(fold change)) < 0.4. **J**. Comparison of canonical pathway enrichments between unnormalized and normalized phosphoproteome. Orange fill colors indicate that all comparable pathways on the top are activated in both omics datasets. The darker the color is, the greater the absolute(z-score) is, and the more significantly enriched the pathway is.

Figure 6. Coordinated regulation of transcriptome, proteome and phosphoproteome on PI3K/AKT signaling. A. Canonical pathway enrichment of phosphoproteome only with cutoff p-value < 0.05. The darker the color is, the greater the absolute(z-score) is, and the more significantly enriched the pathway is. **B**. Comparison of PI3K/AKT signaling and protein ubiquitination pathways enriched from transcriptome (red outline), proteome (blue outline) and phosphoproteome (green outline). **C**. Pathway graph of PI3K/AKT signaling marked with changes in transcriptome (left box), proteome (middle box) and phosphoproteome (right box). Fill colors indicate changes: red and green indicate upregulation and downregulation respectively; grey indicates nonsignificant regulation. **D**. Phosphopeptide number of substrates of PI3K. Y-axis represents protein substates of PI3K; x-axis represents number of phosphopeptides. Red and blue bars indicate upregulated (p-value < 0.05 and log2(fold change) > 0) and downregulated (p-value < 0.05 and log2(fold change) < 0) phosphopeptides respectively.

Figure 7. Activated PI3K/AKT and ERK/MAPK signaling pathways and enhanced protein synthesis and degradation. A-B. Verification of phosphorylation and activation of PI3K/AKT signaling pathway in TGAC8 vs. WT. **C.** Verification of phosphorylation and activation of ERK/MAPK signaling pathway in TGAC8 vs. WT. **D.** Confirmation of enhanced protein synthesis in TGAC8 vs. WT. **E.** The enhanced proteasome activity in TGAC8 vs. WT. **F-G.** The soluble misfolded proteins were increased in TGAC8 LV (**F**) whereas the insoluble protein aggregates did not accumulate within the TGAC8 vs. WT (**G**). Figures **E-G** were adapted from figures in our recently published and closely associated work[10] whose experiments were reproduced in this study.

Figure 8. Analyses of proteins changed discordantly in proteome and phosphoproteome. A. Venn diagram of significantly regulated proteins in total proteome and significantly regulated phosphoproteins in unnormalized phosphoproteome that were conducted concurrently in the same platform. **B-D**.

Functional analyses of proteins whose expressions are changed discordantly at total protein and phosphorylation levels. Mitochondria and others are enriched in cellular component analysis (**B**). Functions related to metabolism, mitochondria and others are enriched in Reactome pathway (**C**) and biological process analyses (**D**).

Figure 9. Deduced schematic of coordination of phosphoproteome with transcriptome and proteome in TGAC8 mouse LV. Based on our results, we deduced a mechanism of reprogramed phosphoproteome in TGAC8 mouse LV: First, TGAC8 mouse induces a PKA dependent phosphorylation via AC8-cAMP-PKA axis. Many cytoplasmic proteins including TFs are thus phosphorylated and then transported into the nuclear where TFs recognize and bind to the promotors to activate the transcription of more regulatory factors, including kinases, phosphatases, and TFs. The activation states of these factors are changed upon phosphorylated in cytosol, thereby activating additional kinases-controlled phosphorylation cascades and reprogramming the cardiac phosphoproteome comprehensively. Left column: AC8-cAMP-PKA signaling; middle column: phosphorylation (phosphoproteome); lower right: transcription (transcriptome); upper right: translation (proteome).

Figure 10. A comprehensive circuitry of the TGAC8 mouse heart concluded from this phosphoproteome combine with previous transcriptome and proteome. Based on the present phosphoproteome, we optimized our previously deduced mechanism graph and labeled findings from the phosphoproteome using red stars. TGAC8 mouse induces a chronic cardiac exercise on heart, manifested as increased heart rate and contractility accompanied with increased energy demand and cardiac biomass. Multiple signaling pathways, related to nutrient sensing, energy production, cardiac cellular stress, cardiac stress response, growth factor signaling, and cell proliferation, are potential downstream mediating the effect of the activated AC8-cAMP-PKA-Ca^{2+} signaling in mouse LV. The altered cardiac functions were also observed associated with protein phosphorylation in our previous study and labeled in blue star here.

Supplementary Figure Legends

Supplementary Figure 1. The enriched pathway, Cardiac Hypertrophy Signaling (Enhanced), from the phosphoproteome. Cardiac Hypertrophy Signaling (Enhanced) is visualized using IPA. Dots with purple outline are identified phosphoproteins or protein complexes. Red and green fill colors indicate upregulation and downregulation respectively.

Supplementary Figure 2. The regulatory pathway under the control of a predicted upstream kinase, PDPK1. PDPK1 in the center is one representative of predicted upstream kinases. Surrounding dots represent identified phosphoproteins differentially regulated in phosphoproteome. Meanings of colors refer to the box of prediction legend besides the graph. Blue glows represent that the increased phosphorylation levels inhibit the activity of corresponding proteins.

Supplementary Figure 3. Phosphopeptide number of substrates of PI3K. Y-axis represents protein substates of PI3K; x-axis represents number of phosphopeptides. Red and blue bars indicate upregulated and downregulated phosphopeptides respectively; green bars indicate nonsignificantly regulated ones. A-B. Red (up): p-value < 0.1 and log2(fold change) > 0; blue (down): p-value < 0.1 and log2(fold change) > 0; green (ns): p-value ≥ 0.1 or log2(fold change) = 0. C. Red (up): p-value < 0.05 and log2(fold change) > 0; blue (down): p-value < 0.05 and log2(fold change) > 0; green (ns): p-value ≥ 0.05 or log2(fold change) = 0.

Figures and Supplementary Figures

Figure 1. TGAC8 reprograms the LV phosphorylation state.

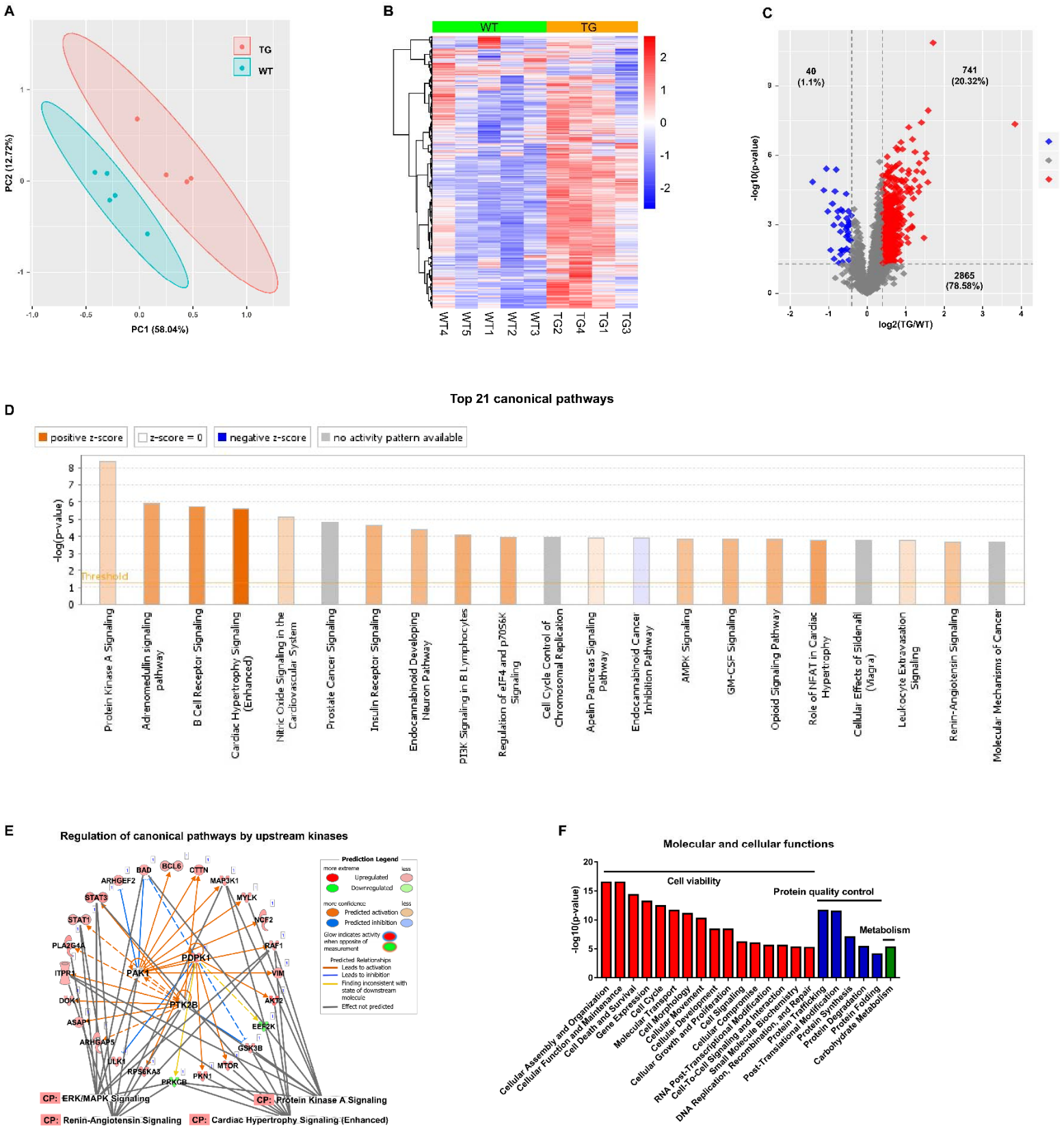

949 **Figure 2. Characteristics of upregulated phosphopeptides.**

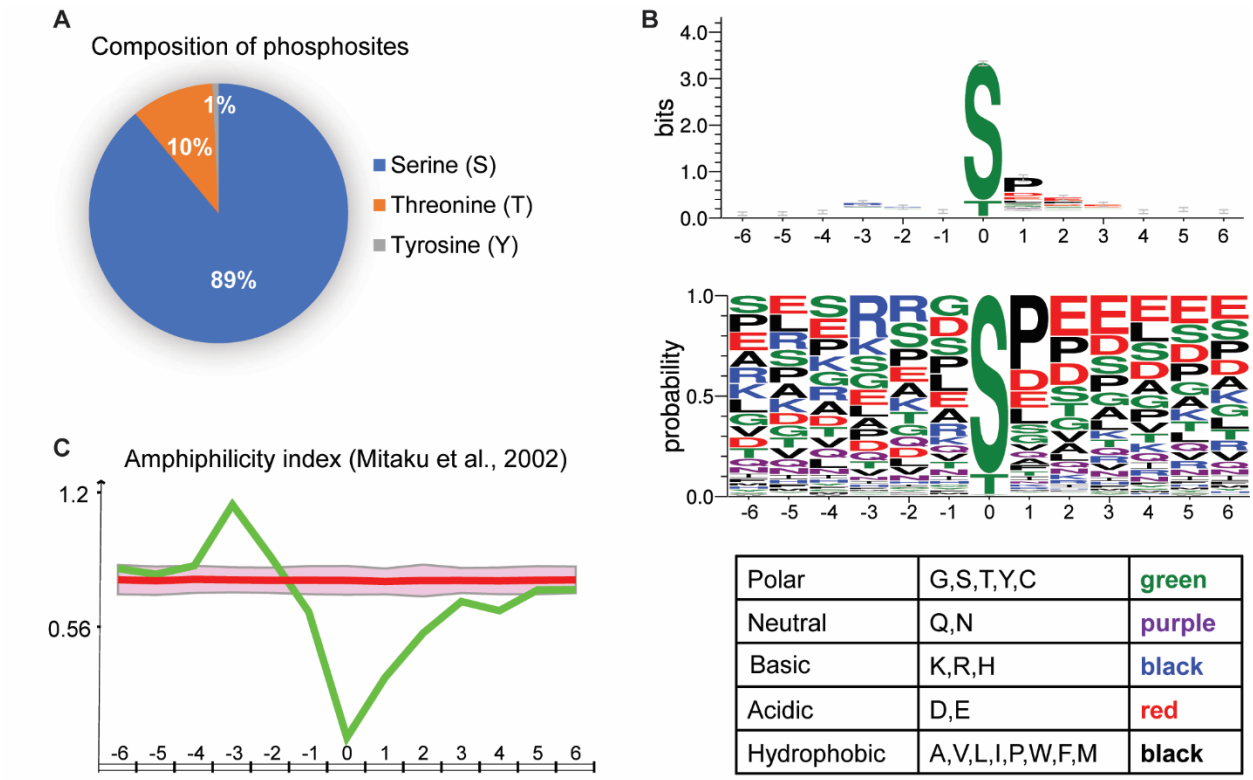

Polar	G,S,T,Y,C	green
Neutral	Q,N	purple
Basic	K,R,H	black
Acidic	D,E	red
Hydrophobic	A,V,L,I,P,W,F,M	black

Figure 3. Integrative analysis of transcriptome, proteome and phosphoproteome.

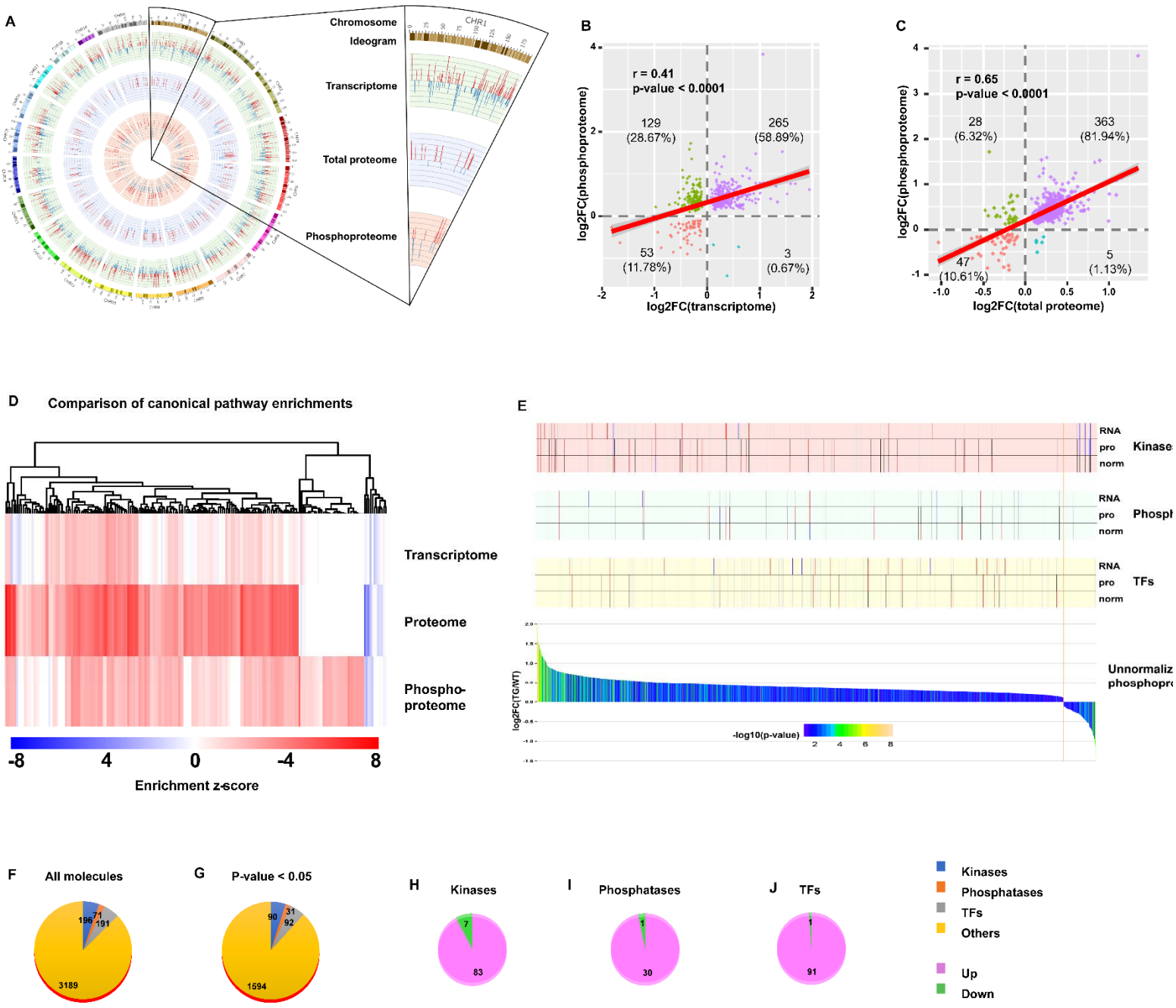

Figure 4. Coordination of phosphoproteome and transcriptome.

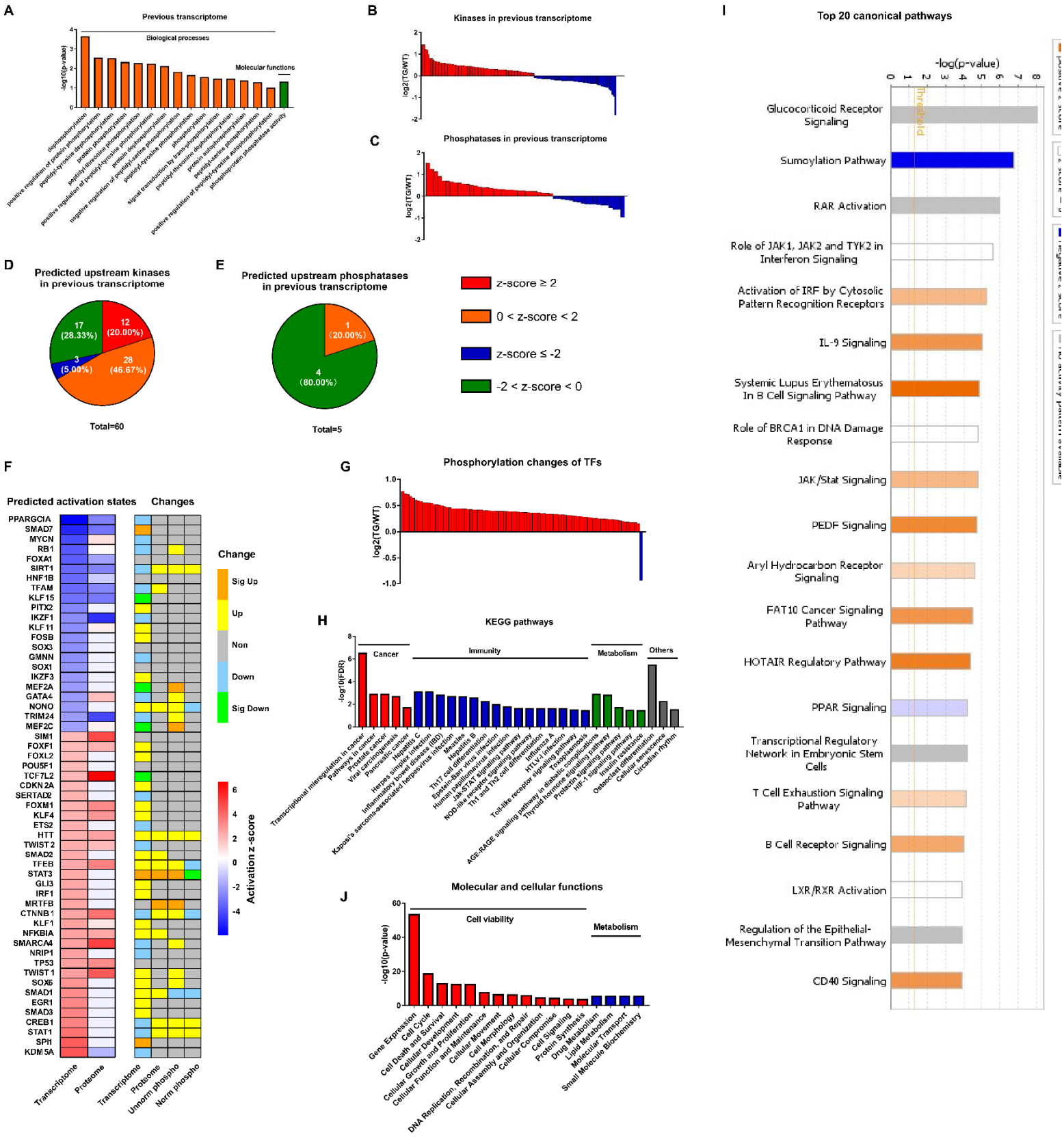

975 **Figure 5. Analysis of normalized phosphoproteome.**

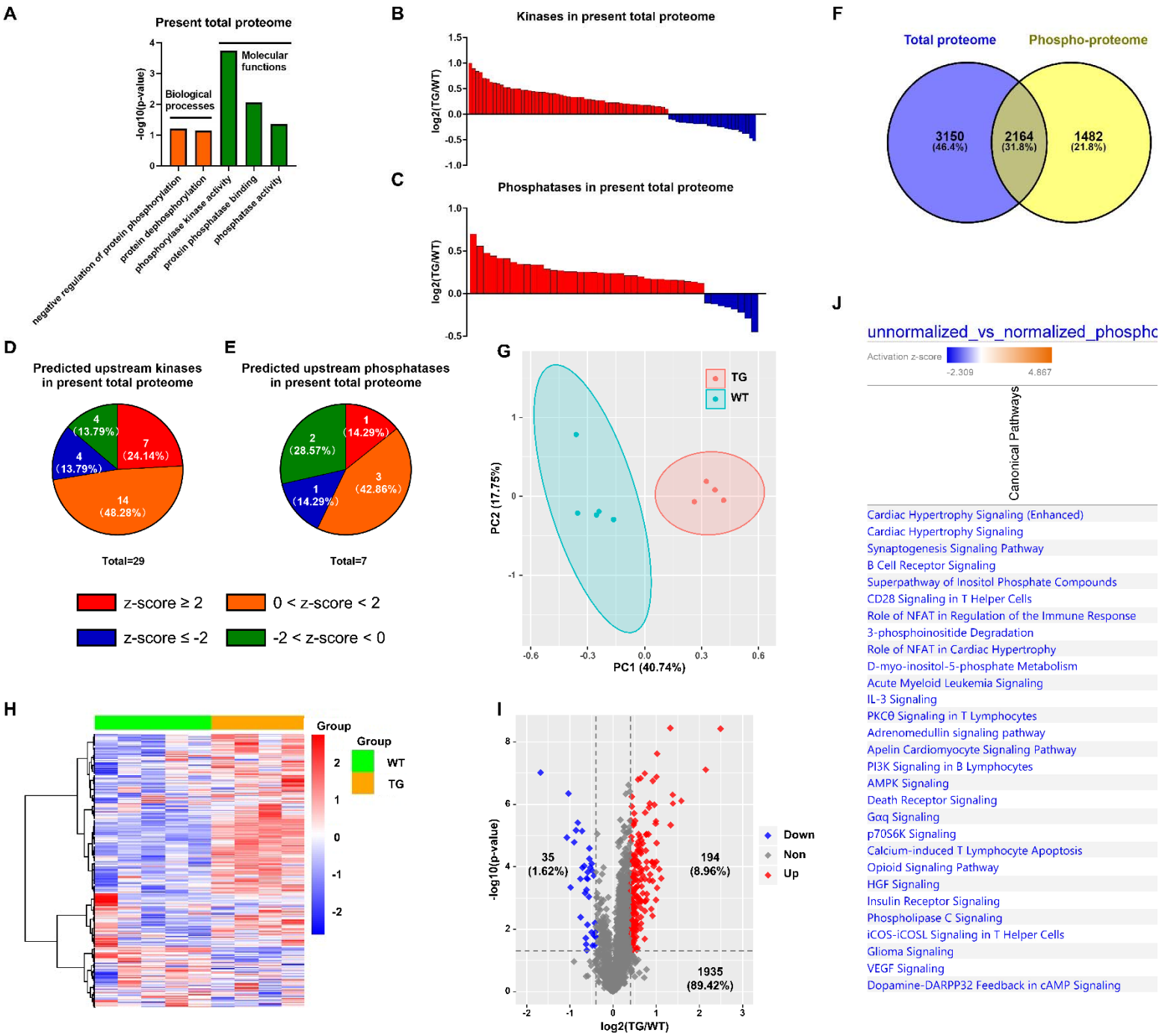

Figure 6. Coordinated regulation of transcriptome, proteome and phosphoproteome on PI3K/AKT signaling.

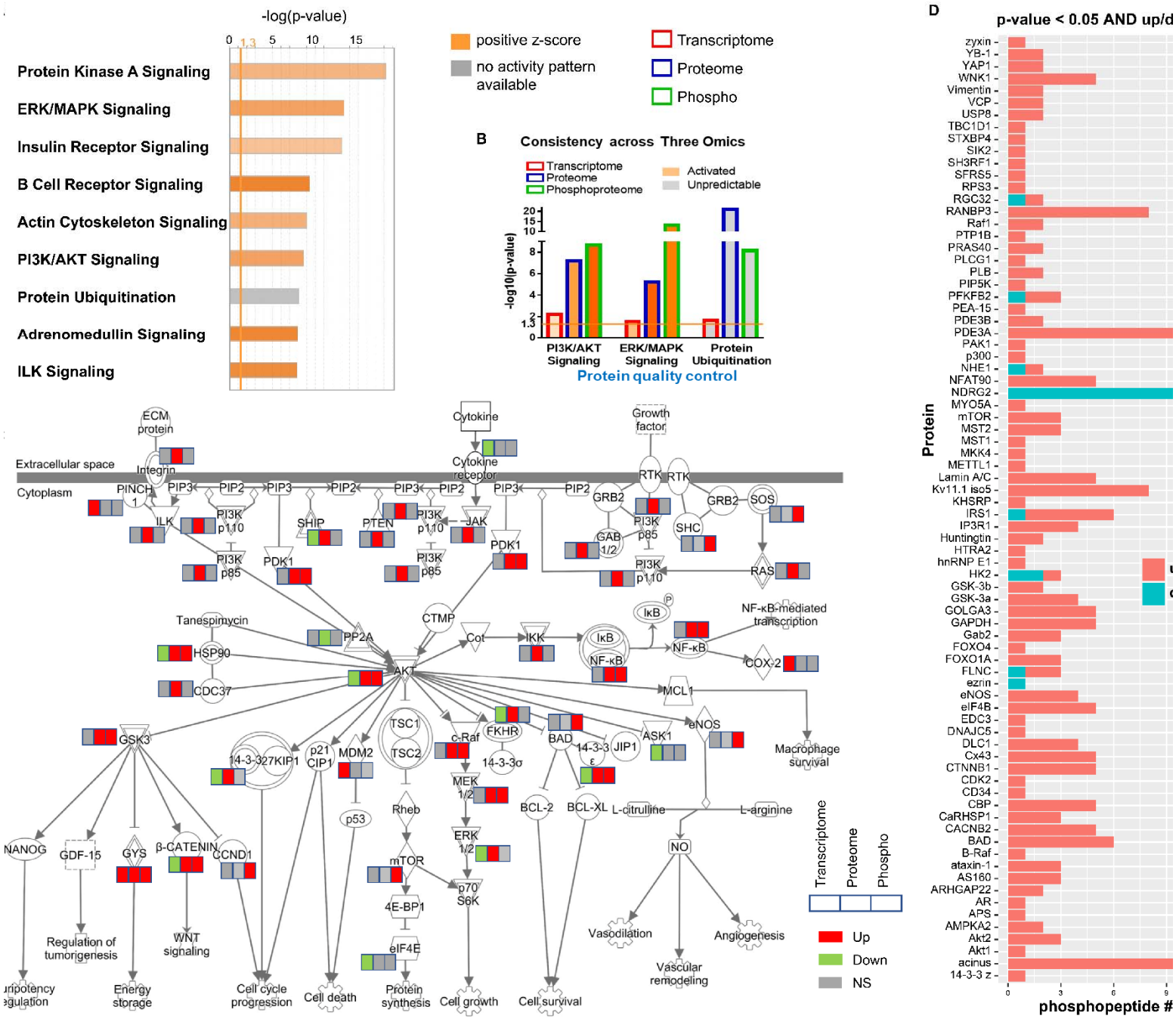

Figure 7. Activated PI3K/AKT and ERK/MAPK signaling pathways and enhanced protein synthesis and degradation.

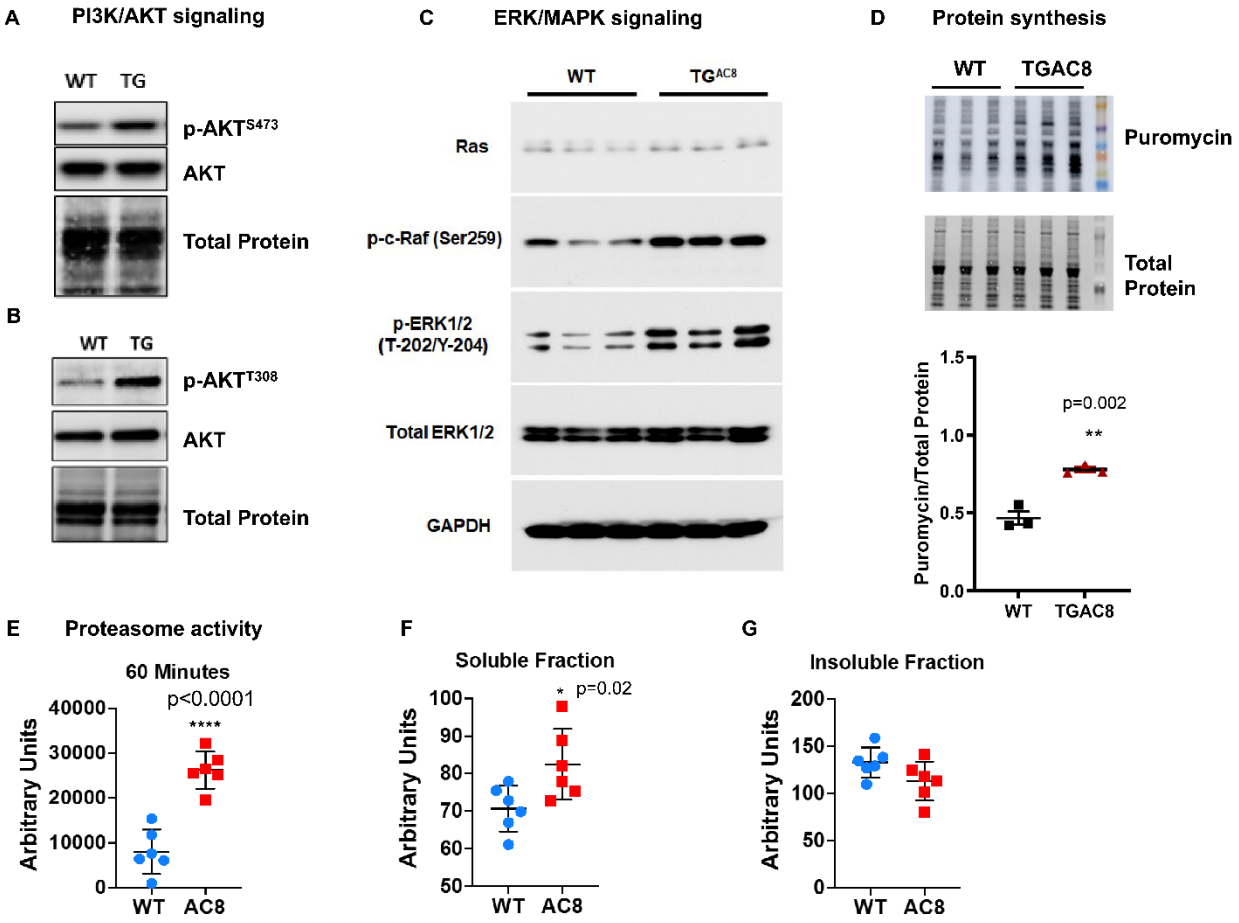

Figure 8. Analyses of proteins changed discordantly in proteome and phosphoproteome.

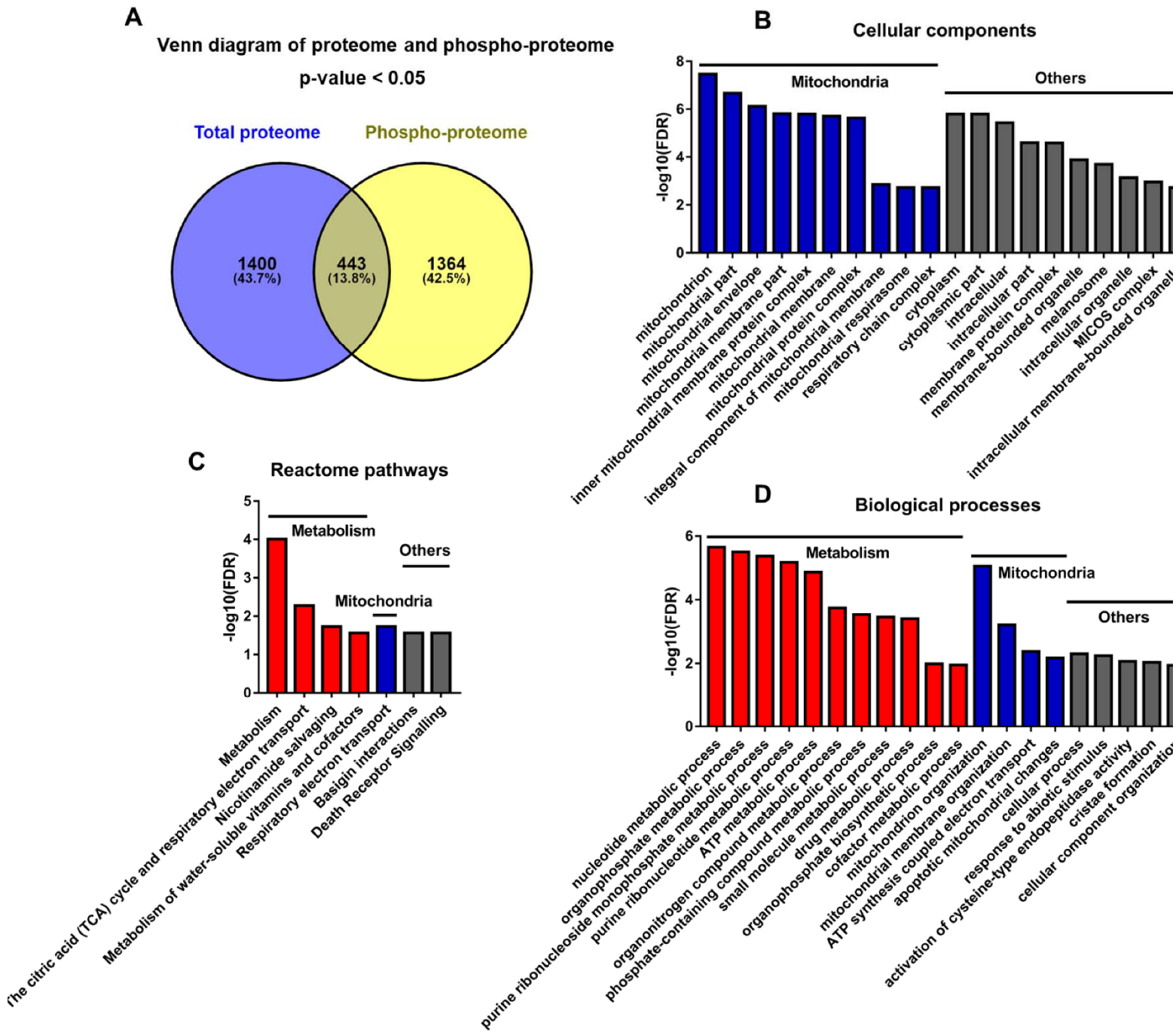

Figure 9. Deduced schematic of coordination of phosphoproteome with transcriptome and proteome in TGAC8 mouse LV.

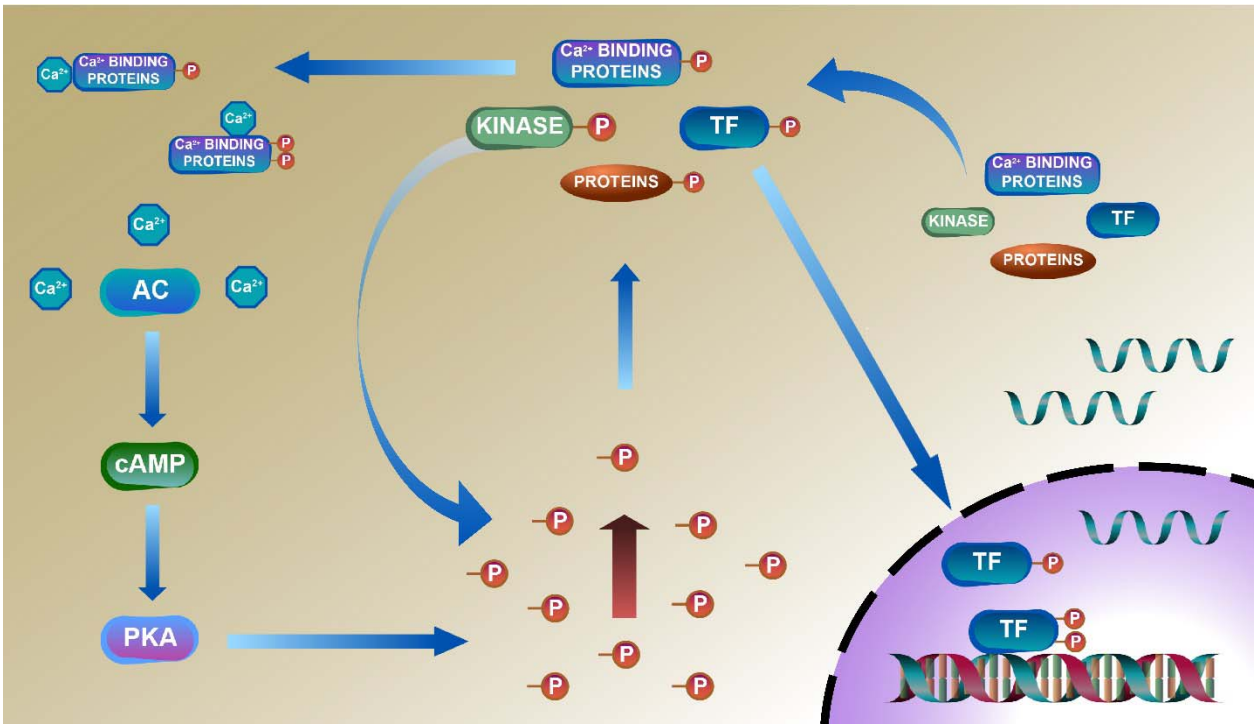

Figure 10. A comprehensive circuitry of TGAC8 mouse heart concluded from this phosphoproteome combine with previous transcriptome and proteome.

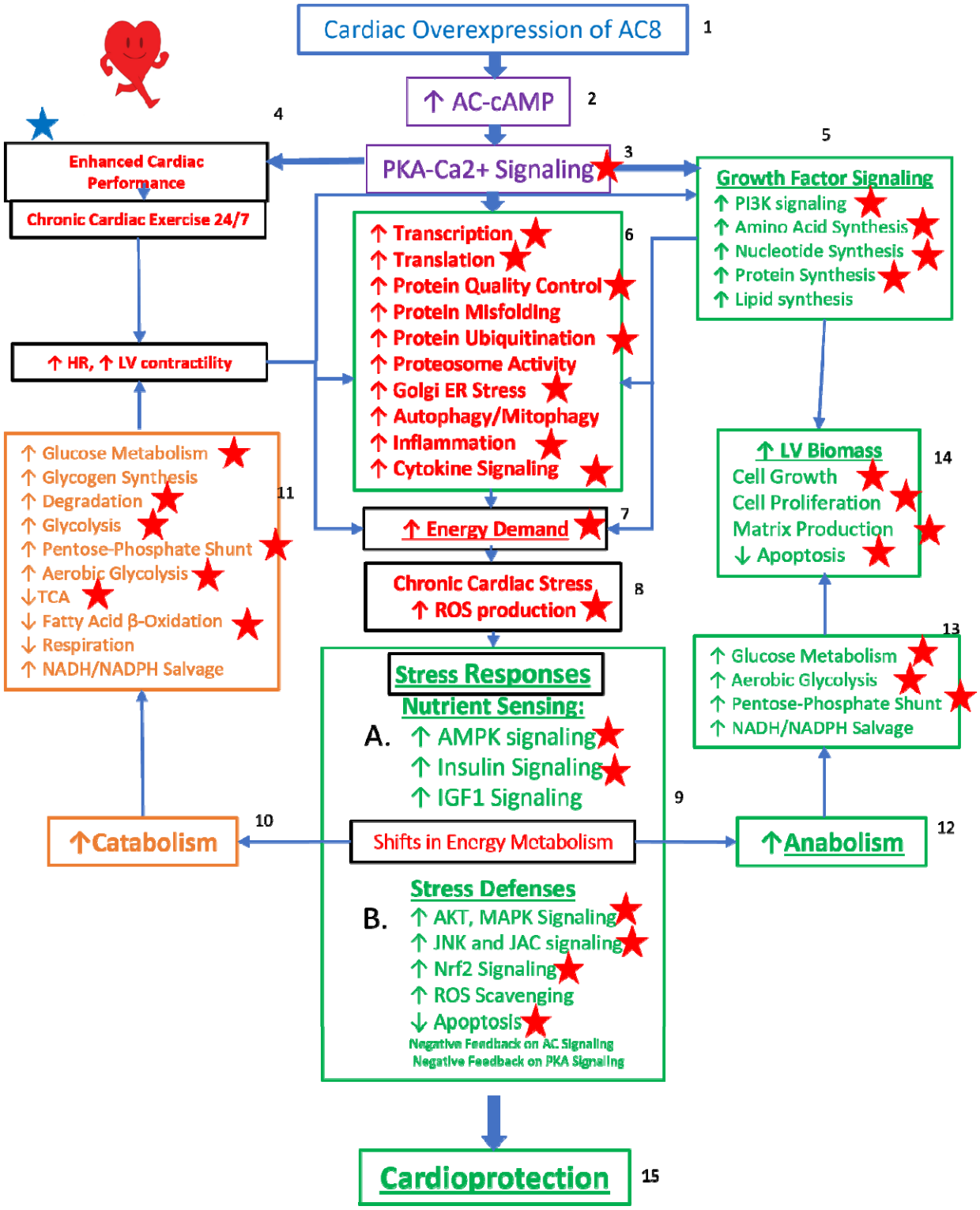

Supplementary Figure 1. The enriched pathway, Cardiac Hypertrophy Signaling (Enhanced), from the phosphoproteome.

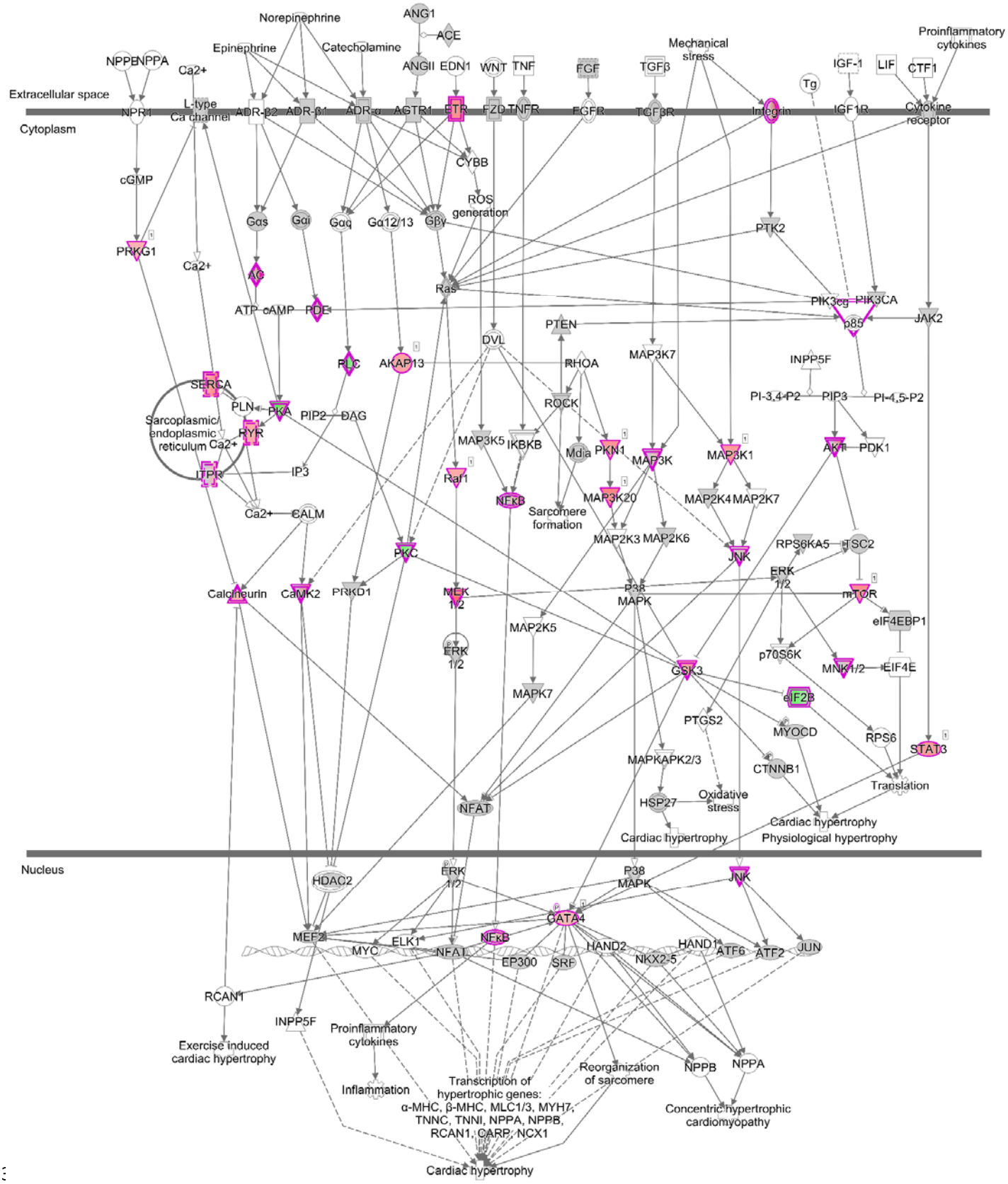
Extracellular space
Cytoplasm
Nucleus
Norepinephrine
Epinephrine
Catecholamine
ANG1
ACE
ANGII
EDN1
WNT
TNF
FGF
TGFβ
Mechanical stress
Proinflammatory cytokines
IGF-1
LIF
CTF1
Tg
NPPB
NPPA
Ca2+
NPR1
L-type Ca channel
ADR-β2
ADR-β1
ADR-α
AGTR1
ETR
FZD
TNFR
EGFR
TGFβR
Integrin
IGF1R
Cytokine receptor
CYBB
ROS generation
cGMP
Gαs
Gαi
Gαq
Gα12/13
Gβγ
PTK2
PRKG1
AC
Ras
ATP
cAMP
PDE
PIK3cg
PIK3CA
p85
JAK2
PTEN
DVL
PLC
AKAP13
RHOA
MAP3K7
INPP5F
SERCA
PLN
PKA
PIP2
DAG
ROCK
PI-3,4-P2
PIP3
PI-4,5-P2
Sarcoplasmic/ endoplasmic reticulum
RYR
MAP3K5
IKBKB
Mdia
PKN1
MAP3K
MAP3K1
AKT
PDK1
ITPR
IP3
Raf1
NFκB
MAP3K20
MAP2K4
MAP2K7
Sarcomere formation
CALM
MAP2K3
MAP2K6
JNK
RPS6KA5
TSC2
PKC
ERK 1/2
Calcineurin
CaMK2
PRKD1
MEK 1/2
P38 MAPK
mTOR
eIF4EBP1
MAP2K5
p70S6K
MNK1/2
EIF4E
GSK3
eIF2B
MAPK7
PTGS2
MYOCD
RPS6
STAT3
MAPKAPK2/3
CTNNB1
Translation
HSP27
Oxidative stress
NFAT
Cardiac hypertrophy
Physiological hypertrophy
HDAC2
GATA4
MEF2
ELK1
MYC
NFAT
EP300
SRF
HAND2
NKX2-5
HAND1
ATF6
ATF2
JUN
RCAN1
Exercise induced cardiac hypertrophy
Proinflammatory cytokines
Inflammation
Transcription of hypertrophic genes: α-MHC, β-MHC, MLC1/3, MYH7, TNNC, TNNI, NPPA, NPPB, RCAN1, CARP, NCX1
Reorganization of sarcomere
Concentric hypertrophic cardiomyopathy

Supplementary Figure 2. The regulatory pathway under the control of a predicted upstream kinase, PDPK1.

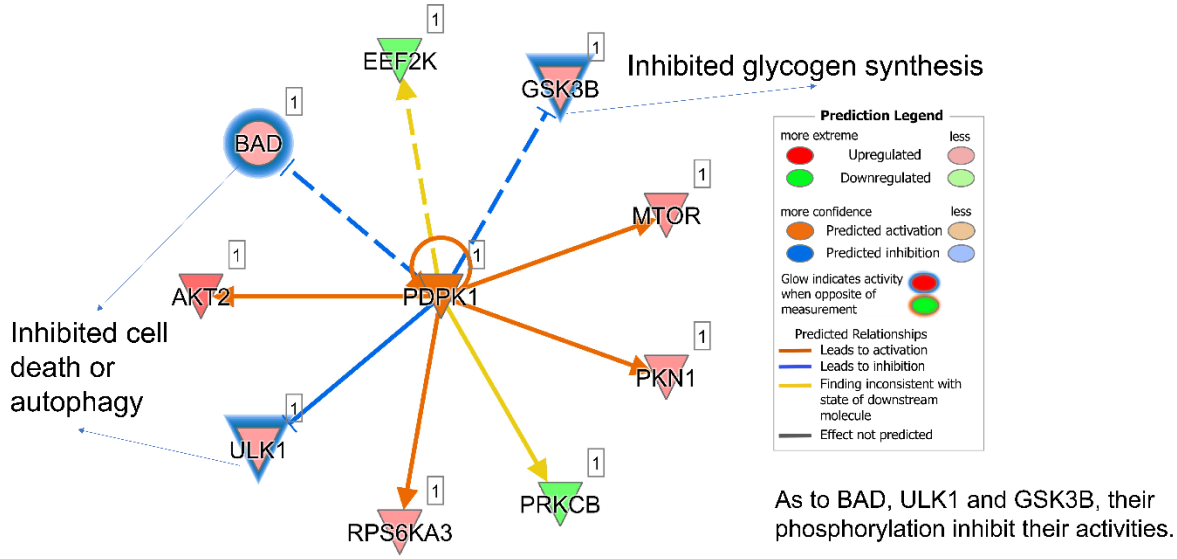

Symbol	Entrez Gene Name	UniProt	Log Ratio	p-value	Location	Family
AKT2	AKT serine/threonine kinase 2	Q60823	0.840825	0.007813	Cytoplasm	kinase
BAD	BCL2 associated agonist of cell death	Q61337	0.476462	7.81E-06	Cytoplasm	other
EEF2K	eukaryotic elongation factor 2 kinase	O08796	-0.42591	0.004744	Cytoplasm	kinase
GSK3B	glycogen synthase kinase 3 beta	Q9WV60	0.556065	0.002741	Nucleus	kinase
MTOR	mechanistic target of rapamycin kinase	Q9JLN9	0.640641	0.000144	Nucleus	kinase
PDPK1	3-phosphoinositide dependent protein kinase 1	Q9Z2A0	0.651174	0.02451	Cytoplasm	kinase
PKN1	protein kinase N1	P70268-2	0.600171	0.007485	Cytoplasm	kinase
PRKCB	protein kinase C beta	P68404-2	-0.44609	0.001011	Cytoplasm	kinase
RPS6KA3	ribosomal protein S6 kinase A3	P18654	0.580733	0.005794	Cytoplasm	kinase
ULK1	unc-51 like autophagy activating kinase 1	O70405	0.549454	0.015177	Cytoplasm	kinase
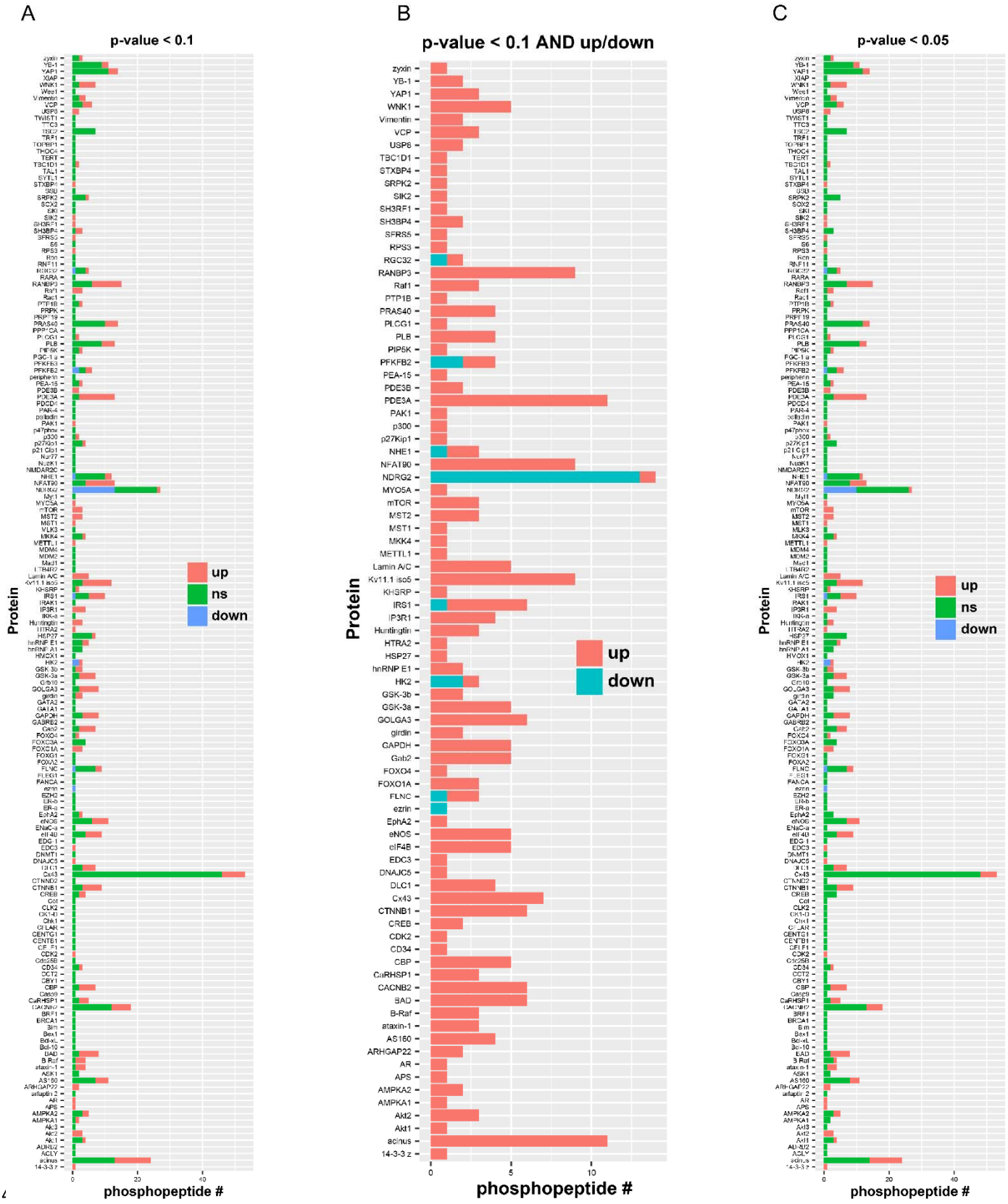
Supplementary Figure 3. Phosphopeptide number of substrates of PI3K.